Journal for ImmunoTherapy of Cancer

Targeting CISH enhances natural cytotoxicity receptor signaling and reduces NK cell exhaustion to improve solid tumor immunity

Pierre-Louis Bernard,[1] Rebecca Delconte ,[2] Sonia Pastor,[1] Vladimir Laletin ,[1] Cathy Costa Da Silva,[1] Armelle Goubard,[1] Emmanuelle Josselin,[1] Rémy Castellano ,[1] Adrien Krug,[3] Julien Vernerey ,[1] Raynier Devillier ,[1] Daniel Olive ,[1] Els Verhoeyen ,[3] Eric Vivier ,[4] Nicholas D Huntington ,[5] Jacques Nunes ,[1] Geoffrey Guittard [1]

To cite: Bernard P-L, Delconte R, Pastor S, *et al*. Targeting CISH enhances natural cytotoxicity receptor signaling and reduces NK cell exhaustion to improve solid tumor immunity. *Journal for ImmunoTherapy of Cancer* 2022;**10**:e004244. doi:10.1136/jitc-2021-004244

► Additional supplemental material is published online only. To view, please visit the journal online (http://dx.doi.org/10.1136/jitc-2021-004244).

JN and GG contributed equally.

Accepted 06 April 2022

For numbered affiliations see end of article.

Correspondence to
Dr Geoffrey Guittard;
geoffrey.guittard@inserm.fr

ABSTRACT

Background The success and limitations of current immunotherapies have pushed research toward the development of alternative approaches and the possibility to manipulate other cytotoxic immune cells such as natural killer (NK) cells. Here, we targeted an intracellular inhibiting protein 'cytokine inducible SH2-containing protein' (CISH) in NK cells to evaluate the impact on their functions and antitumor properties.

Methods To further understand CISH functions in NK cells, we developed a conditional Cish-deficient mouse model in NK cells (*Cish*$^{fl/fl}$*Ncr1*$^{Ki/+}$). NK cells cytokine expression, signaling and cytotoxicity has been evaluated in vitro. Using intravenous injection of B16F10 melanoma cell line and EO711 triple negative breast cancer cell line, metastasis evaluation was performed. Then, orthotopic implantation of breast tumors was performed and tumor growth was followed using bioluminescence. Infiltration and phenotype of NK cells in the tumor was evaluated. Finally, we targeted *CISH* in human NK-92 or primary NK cells, using a technology combining the CRISPR(i)-dCas9 tool with a new lentiviral pseudotype. We then tested human NK cells functions.

Results In *Cish*$^{fl/fl}$*Ncr1*$^{Ki/+}$ mice, we detected no developmental or homeostatic difference in NK cells. Global gene expression of *Cish*$^{fl/fl}$*Ncr1*$^{Ki/+}$ NK cells compared with *Cish*$^{+/+}$*Ncr1*$^{Ki/+}$ NK cells revealed upregulation of pathways and genes associated with NK cell cycling and activation. We show that CISH does not only regulate interleukin-15 (IL-15) signaling pathways but also natural cytotoxicity receptors (NCR) pathways, triggering CISH protein expression. Primed *Cish*$^{fl/fl}$*Ncr1*$^{Ki/+}$ NK cells display increased activation upon NCR stimulation. *Cish*$^{fl/fl}$*Ncr1*$^{Ki/+}$ NK cells display lower activation thresholds and *Cish*$^{fl/fl}$*Ncr1*$^{Ki/+}$ mice are more resistant to tumor metastasis and to primary breast cancer growth. CISH deletion favors NK cell accumulation to the primary tumor, optimizes NK cell killing properties and decreases TIGIT immune checkpoint receptor expression, limiting NK cell exhaustion. Finally, using CRISPRi, we then targeted *CISH* in human NK-92 or primary NK cells. In human NK cells, CISH deletion also favors NCR signaling and antitumor functions.

Conclusion This study represents a crucial step in the mechanistic understanding and safety of *Cish* targeting to unleash NK cell antitumor function in solid tumors. Our results validate CISH as an emerging therapeutic target to enhance NK cell immunotherapy.

Key messages

⇒ The success and limitations of current immunotherapies have pushed research toward the development of alternative approaches and the possibility to manipulate other cytotoxic immune cells such as natural killer (NK) cells. Targeting cytokine inducible SH2-containing protein (CISH) inhibiting protein in NK cells improves ex vivo proliferation, functions and signaling activation of several pathways such as cytokines and NK activating receptors. In vivo CISH absence favors NK cells infiltration to the tumor burden, optimize their killing properties and limits NK cells exhaustion. Consequently, primary tumor and metastasis development are greatly impaired in preclinical mouse model. Finally, we targeted CISH in human NK-92 or primary NK cells, using a technology combining the CRISPR(i)-dCas9 tool with a new lentiviral pseudotype, this, improving their function. Our results validate CISH as an emerging therapeutic target to enhance NK cell immunotherapy.

BACKGROUND

Immunotherapy strategies aim to mobilize the patient's immune defenses against his tumor cells,targeting in particular cytotoxic effectors (CD8$^+$ T cells, γδ T cells and natural killer (NK) cells). These new therapies are mainly targeting CD8$^+$ T cells and have a significant impact on the prognosis and survival of patients with cancer. However, many patients are refractory to these treatments. The success and limitations of current immunotherapies have pushed research

toward the development of alternative approaches and the possibility to manipulate other cytotoxic immune cells such as NK cells.

NK cells receive a renewed interest in immunotherapy because they do not rely on antigen specificity like $CD8^+$ T cells, hence displaying a broader reactivity to tumors.[1–3] The distinction between a healthy cell (to be spared) and a malignant cell (undesirable) is possible thanks to a panel of inhibitory and activating surface receptors capable of integrating danger signals. NK cells also play a critical role in helping innate and adaptive immune responses via cellular cross-talk in various disease settings.[4] Finally, in an adoptive transfer therapy setting, NK cells have greater off-the-shelf utility and are safer. Indeed, these cells are less persistent reducing the risk of autoimmunity and side effects such as cytokine storms (cytokine-release syndrome) that may result from an over activation of T cells. Therefore, therapeutic approaches that trigger and/or reconstitute NK cell function and proliferation are crucial in tumor immunotherapy. In addition, NK cells engineered with chimeric antigen receptor, targeting tumor antigens, are highly promising.[5]

In numerous preclinical studies, NK cells have shown an ability to limit the metastatic spread of experimental and spontaneous tumors.[6 7] In clinical settings, NK cell activity has been inversely correlated with cancer incidence, [8] and several studies show that NK cell infiltration in lung, gastric, neuroblastoma and colorectal cancers is associated with better patient outcomes.[1 9]

Targeting inhibitory intracellular proteins, such as Cytokine inducible SH2-containing protein (CISH), a member of the SOCS (Suppressor of Cytokine Signaling) family, can be effective in enhancing $CD8^+$ T cell tumor immunity in preclinical models.[10 11] These studies led to a clinical trial protocol NCT04426669. CISH has been also shown to be a critical immune checkpoint in NK cells[12] and we recently contributed to show the importance of CISH in NK cell homeostasis using a *Cish* KO germline mouse model.[13] However, we still do not fully appreciate mechanistically how CISH regulates NK antitumor functions. These are essential requirements to comprehensively uncover the safety of genetically or pharmacologically targeting an intracellular protein in NK cell immunotherapy.

To further understand how CISH regulates NK cell activity, we developed and investigated a new conditional mouse model that depletes CISH specifically in NK cells ($Cish^{fl/fl}Ncr1^{iCre}$) and targeted *CISH* in human NK cells using a CRISPRi method. This study represents a crucial step in the mechanistic understanding and safety of *Cish*-targeting to unleash NK cell antitumor function in solid tumors.

METHODS

Mice

Generation and genotyping of Tm1c $Cish^{fl/fl}$ mice are descripted in online supplemental material. Tm1c $Cish^{fl/fl}$ mice were then crossed with $Ncr1^{iCre/+}$ mice.[14] Mice were bred and maintained under specific pathogen-free conditions at the Center de Recherche en Cancérologie de Marseille (CRCM) animal facility. Animal experiments followed were performed in accordance with institutional committees and French and European guidelines for animal care.

NK cell expansion

NK cells were purified from mouse spleens using Mouse NK cell isolation Kit according to manufacturer's specifications (STEMCELL #19855). NK cells were then expanded for 6 days with hIL-15 50 ng/mL (Miltenyi #130-095-765) in RPMI 20% FCS supplemented with L-glutamine (2 mM; Gibco), penicillin/streptomycin (100 µg/mL; Gibco), Sodium Pyruvate (1 mM; Gibco) and finally FACS sorted ($NK1.1^+$, $NKp46^+$, $CD3^-$, $CD19^-$) (BD Biosciences FACSAria III). After overnight starvation in the absence of IL-15, $Cish^{+/+}Ncr1$ iCre or $Cish^{fl/fl}Ncr1^{iCre}$ NK cells were stimulated or not during 4 hours with IL-2 (Proleukin, Novartis pharma SAS) or IL-15.

NK cell cytotoxicity assays

Standard 4 hours cytotoxicity assays were completed as described elsewhere[15] and described in online supplemental material.

Proliferation assay

For assessment of cellular proliferation by CFSE (carboxy fluorescein diacetate succinimidyl diester; Life Technologies #C34554), splenic NK cells were purified from $Cish^{+/+}Ncr1$ iCre or $Cish^{fl/fl}Ncr1^{iCre}$ mice, then labeled with 0.1 µM CFSE and cultured with various doses of hIL-15 for 5 days, before flow cytometric analysis.

Cytokine assay

For the measurement of IFN-γ production, splenocytes were activated in 96 well plates with hIL-15 (50 ng/mL), IL-12 (10 ng/mL, Peprotech), IL-18 (100 ng/mL), PMA (10 ng/mL), Ionomycin (1 µg/mL), or coated with anti-NK1.1 (25 µg/ml, BioLegend), anti-NKp46 (10 µg/mL, BioLegend) or NKG2D (10 µg/mL, BioLegend). Cells were incubated with monensin and brefeldin A (BD GolgiPlug and GolgiStop) in complete medium for 4 hours at 37°C. The cells were subjected to surface staining and intracellular staining was performed by use of the FoxP3/Transcription Factor Staining Buffer Set (eBioscience).

Experimental tumor experiments

Single-cell suspensions of 3×10^5 B16F10 melanoma cells were injected intravenous into the tail vein of the indicated strains of mice. Mice were sacrificed and lungs were harvested on day 14. Lungs from B16F10 injected mice were fixed in PFA 4% overnight to count B16F10 metastases. E0771-GFP^+-Luciferase breast cancer cells were injected into the tail vein of the indicated strains of mice (5×10^5 cells/mouse). Luciferase expression was then monitored at day 7 and 14 by bioluminescence using PhotonIMAGER (BiospaceLab), following intraperitoneal injection of luciferin (30 mg/kg). After completion

of the analysis organ luminescence was assessed. Orthotopic implantation of breast tumors and tumor dissociation was performed as previously described.[16] Luciferase expression was monitored by bioluminescence using PhotonIMAGER (BiospaceLab), after intraperitoneal injection of luciferin (30 mg/kg).

Sample preparation, RNA sequencing and bioinformatics analysis

RNA isolation from sorted ex vivo NK cells was extracted using the RNeasy Plus mini Kit (#74134, QIAGEN, Hilden, Germany), according to the manufacturer's instructions. Purified RNA was measured using an Agilent 2200 TapeStation System (Agilent) with high sensitivity RNA ScreenTapes (#5067-5579, Agilent).

Primary NK cell cultures

Peripheral blood mononuclear cells (PBMCs) were obtained by centrifugation on density gradient of whole blood from healthy volunteers (HV) provided by the local Blood Bank (Etablissement Francais du Sang). Human NK cells were isolated from PBMCs obtained from multiple different HVs. Negative selection of NK was performed on EasySep Human NK Cell Enrichment Kit system (StemCell Technologies). 2×10^6sorted NK cells were cultured with 100 Gy-irradiated EBV-LCL cells in a 1:20 ratio, in 20 mL of RPMI supplemented with 10% fetal bovine, 1X GlutaMAX (both from Gibco) and 500 UI/mL IL-2 (Proleukin, Novartis).

NK-92 and primary NK cells transduction

Transduction was performed as previously described and detailed in online supplemental material.[17] After production, concentrated viruses were added at the indicated MOI (multiplicity of infection) in presence of retronectin at 10 µg/mL (Takara). The plates were then centrifuged at 1000 g for 1 hour and incubated at 37°C during 3 hours. NK-92 or primary NK cells were then added at 1. A 10^6 cells/mL in 500 µL of regular medium supplemented with IL-2 500 UI in presence of protamine-sulfate at 20 µg/mL (Sigma). The plates were then centrifuged at 1000 g for 1 hour and incubated at 37°C overnight. The next day, IL-2-supplemented medium was added to each well. Transduction was assessed by cytometry on day 7 after transduction. NK-92 or primary NK cells were then sorted using the the BD FACSAria III Cell Sorter sorting mCherry and GFP positive cells.

RESULTS

Deletion of CISH in mature NK cells does not impact maturation

To develop a conditional *Cish*-deficient mouse, we developed $Cish^{fl/fl}$ mice that were then bred with the $Ncr1^{iCre}$ transgenic mice to induce deletion of *Cish* in NK cells (online supplemental figure 1A). Efficient deletion of CISH was first confirmed by western blot (WB) and showed no evidence of CISH in purified and expanded splenic NK cells stimulated with IL-2 or IL-15 (online supplemental figure 1B). Similar to germline *Cish*-deleted mice, $Cish^{fl/fl}Ncr1^{iCre}$ mice were healthy, fertile and contained equivalent frequencies and numbers of NK cells in bone marrow and spleen (online supplemental figure 1C–E).

To determine whether *Cish*-deletion in NK cells perturbs their biology, we assessed the phenotype of NK cells that were *cish*-deleted. Natural cytotoxicity receptors (NCR), CD122 (IL-15Rβ) and DNAM1 receptors expressions are normal (online supplemental figure 2A–C). The maturation of $Cish^{fl/fl}Ncr1^{iCre}$ NK cells is also normal showing equivalent frequencies of immature, M1 and M2 NK cell populations (figure 1A,B) (online supplemental figure 2D,E). Altogether, we did not notice any phenotypical differences in $Cish^{fl/fl}Ncr1^{iCre}$ NK cells.

CISH depletion reveals upregulation of pathways and genes associated with NK cell-cycling and activation

We next compared the gene expression profiles of $Cish^{+/+}Ncr1^{iCre}$ vs $Cish^{fl/fl}Ncr1^{iCre}$ NK cells. Cells from spleen were purified and analyzed by RNAseq. After *Cish* deletion, more than 200 genes were differentially expressed (±20% expression, adjusted p value ≤5%). Among them, about 60 genes have a modulated expression of a fold increase greater than 2 (figure 1C). An analysis by KEGG and GO enrichment highlighted signaling pathways such as cell cycle progression, cytokine signaling or NK activating receptors. This, allowed us to assess the influence of the absence of *Cish* on these biological processes and to determine the putative markers responsible for these perturbations (figure 1D–F). Overall $Cish^{fl/fl}Ncr1^{iCre}$ cells appeared to display a more-activated phenotype than their $Cish^{+/+}Ncr1^{iCre}$ counterparts.

CISH depletion favors IL-15 cytokine signaling pathway decreasing NK activation threshold

Following IL-15 stimulation, *Cish*-depleted NK cells exhibited an increased proliferation compared with $Cish^{+/+}Ncr1^{iCre}$ cells (figure 2A,B). Interestingly, $Cish^{fl/fl}Ncr1^{iCre}$ cells proliferate efficiently at IL-15 doses as low as 10 ng/mL. $Cish^{fl/fl}Ncr1^{iCre}$ cells showed max proliferation rate at 30 ng/mL of IL-15, whereas $Cish^{+/+}Ncr1^{iCre}$ cells needed at least 50 ng/mL. $Cish^{fl/fl}Ncr1^{iCre}$ NK cells are thus more sensitive to IL-15 and their activation threshold is greatly diminished. On IL-15 activation CD122 expression decreased in both conditions but remained higher in a $Cish^{fl/fl}Ncr1^{iCre}$ NK cells compared with $Cish^{+/+}Ncr1^{iCre}$ at day 6 (figure 2C). This suggests a role for CISH in the recycling and degradation of CD122 receptor. IL-15-stimulated *Cish*-deficient NK cells showed also improved IFN-γ and CD107a expression (figure 2D,E).

CISH is expressed on NCRs stimulation but mildly affected naïve NK cell functions and signaling

We next tested CISH expression upon cytokine stimulation. As expected, CISH expression is induced after 4 hours of IL-2 or IL-15 stimulation (figure 3A). NK cells express a variety of receptors that allow them to detect

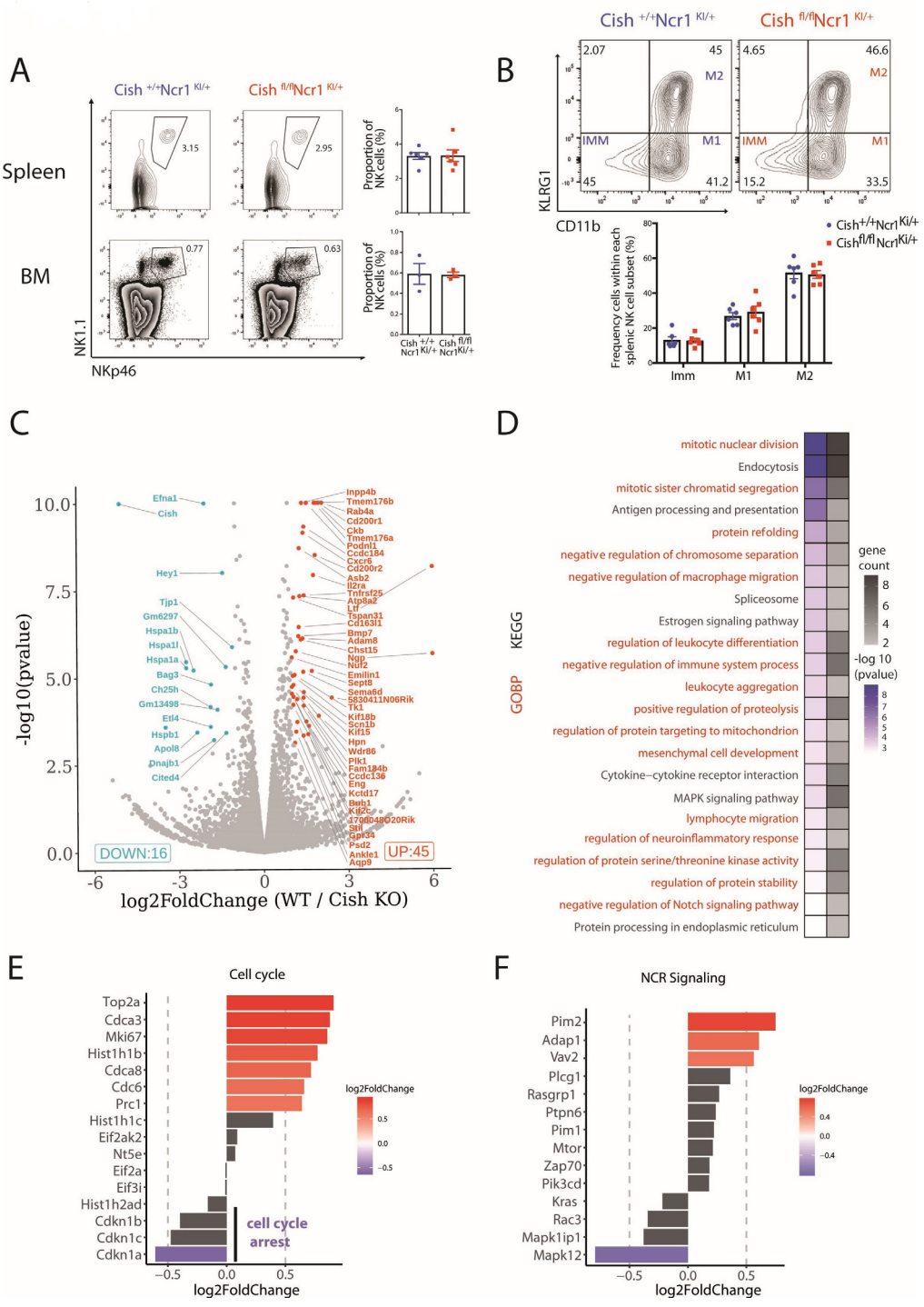

Figure 1 Deletion of *Cish* gene does not impact NK cell maturation but reveals upregulation of pathways in cell cycling and activation. (A, B) BM and/or splenic NK cells from *Cish* $^{+/+}$*Ncr1*$^{Ki/+}$ and *Cish* $^{fl/fl}$*Ncr1*$^{Ki/+}$ mice were phenotypically analyzed by FACS. (A) Frequency of NK cells in spleen and bone marrow (CD3$^-$, CD19$^-$, NK1.1$^+$, NKp46$^+$), representative FACS plots and histograms are shown. (B) Frequency of Imm, M1 and M2 cells were measured within NK cell populations from the spleen, representative FACS plots and histograms are shown. (C, F) Gene expression profiles of FACS sorted NK cells (NK1.1$^+$, NKp46$^+$, CD3$^-$) were generated using RNA-sequencing. (C) A volcano plot of the top 60 significant ($p<0.05$) differentially expressed genes with a fold change above +1 or below –1 was generated. The y-axis is the negative log-p value and x-axis is the log-fold-change of the corresponding gene in *Cish*$^{-/-}$ vs *Cish*$^{+/+}$ comparison. Gene expression: blue=downregulated, red=upregulated. (D) Heatmap showing results of gene ontology analysis for genes in *Cish*$^{-/-}$ vs *Cish*$^{+/+}$ comparison (From KEGG pathway analysis in black or GOBP in red), log-p value are indicated in blue color gradient and gene count in black color gradient. An upregulated list of genes associated with cell cycle (E) and natural cytotoxicity receptor pathways (F) (from KEGG pathway analysis) was generated with a *p* value cut-off of <0.05. x-axis is the log(FC) of each gene and *p* values are indicated by color. BM, bone marrow; GOPB, gene ontology biological process; KEGG, Kyoto Encyclopedia of Genes and Genomes; NCR, natural cytotoxicity receptor; NK, natural killer.

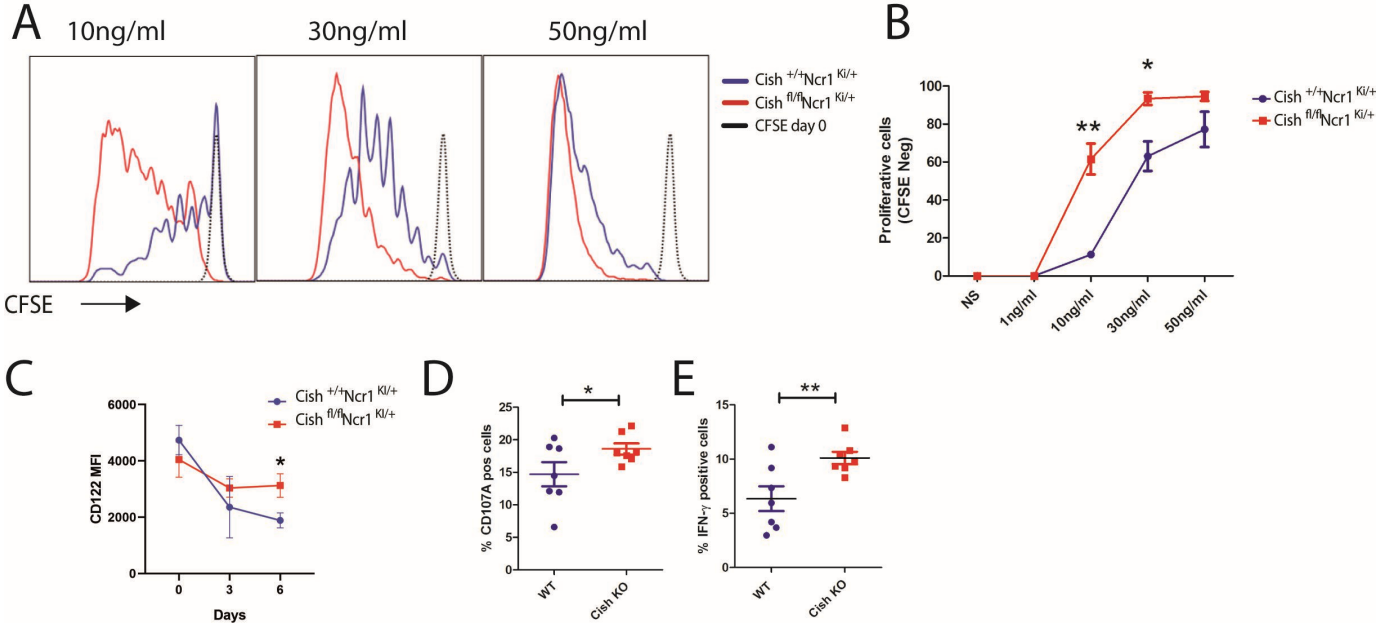

Figure 2 CISH depletion favors IL-15 cytokine signaling pathway. (A, B) FACS analysis of *Cish* $^{+/+}$*Ncr1*$^{Ki/+}$ and *Cish* $^{fl/fl}$*Ncr1*$^{Ki/+}$ purified NK cells labeled with CFSE and cultured for 6 d in IL-15 (10–50 ng/mL). (A) Representative FACS plot is showed. (B) Representative curve using cells from 3 mice and two independent experiments are shown. (C) FACS was used to quantify the MFI of CD122 at different time points on *Cish* $^{+/+}$*Ncr1*$^{Ki/+}$ and *Cish* $^{fl/fl}$*Ncr1*$^{Ki/+}$ NK cells. (C) Representative curve of 3 different experiments are shown. (D, E) Histograms using cells from 6 mice and two independent experiments showing Flow cytometric analysis of IFN-γ production (D) and CD107a (LAMP-1) (E) expression *Cish* $^{+/+}$*Ncr1*$^{Ki/+}$ and *Cish* $^{fl/fl}$*Ncr1*$^{Ki/+}$ NK cells from splenocytes cultured for 4 hours in IL-15 (50 ng/mL). *P<0.05, **p<0.01 (Student's t-test). CFSE, carboxyfluorescein succinimidyl ester; CISH, cytokine inducible SH2-containing protein; NK, natural killer.

target cells (endangered, infected or tumor cells) while sparing normal cells.[18] This recognition is performed via a multitude of activating receptors (NKRs) such as the NCRs, NKG2D, 2B4, DNAM-1 or the Fc fragment receptor for immunoglobulins, CD16 (FcRIIA).[3] We hypothesized that CISH could be involved in the signal encoded by NCR engagement as suggested by RNA-seq analysis (figure 1F). CISH was induced following stimulation with NKG2D, NKp30 or NKp46, respectively in a human NK lineage (NK-92) and naive mouse NK cells (figure 3B,C). These receptors and the integrity of their signaling pathways are essential for the recognition and subsequent elimination of a tumor cell.

We next decided to test NK cell cytokine expression upon NKRs activation. Prior to this, we confirmed that there is no difference in NKRs expression between *Cish*$^{+/+}$*Ncr1* ^{iCre} and *Cish*$^{fl/fl}$*Ncr1*^{iCre} NK cells (online supplemental figure 2C). Spleen purified naïve NK cells were stimulated with plate bound indicated NKRs (figure 3D). We detected no statistical difference in IFN-γ expression. The same results were obtained with stronger stimulations such as PMA (phorbol myristate acetate) and ionomycin (online supplemental figure 3A). Then, phosphoflow analyses were performed after short NKRs cross-linking or PMA/Ionomycin stimulation showing no statistical difference in phospho-ERK (figure 3E,G) (online supplemental figure 3B). Naïve *Cish*$^{+/+}$*Ncr1* ^{iCre} and *Cish*$^{fl/fl}$*Ncr1*^{iCre} NK cells responded equivalently to NKRs stimulations.

CISH deletion favors ex vivo expanded NK cell signalling, proliferation and functions

As activated NK cells are more susceptible to express CISH, we performed activation and amplification of splenic murine NK cells during 6 days (LAKs; Lymphokine-activated killer cells).[19] At day 6, total LAK cells is increased in *Cish*$^{fl/fl}$*Ncr1*^{iCre} compared with *Cish*$^{+/+}$*Ncr1* ^{iCre} genotype (figure 4A). In absence of CISH, twice the total absolute number of NK cells was produced (figure 4B). At day 6, there are more NK and NKT cells in *Cish*$^{fl/fl}$*Ncr1*^{iCre} cultures and as a counterpart a dramatic decrease in T cell proportion (figure 4C). NK and NKT cells both express NKp46 receptor and are thus Cish-deficient in *Cish*$^{fl/fl}$*Ncr1*^{iCre} mice.

We next decided to test whether *Cish*$^{fl/fl}$*Ncr1*^{iCre} NK cells were more sensitive to NKRs (NKp46, NK1.1, NKG2D) than their *Cish*$^{+/+}$*Ncr1* ^{iCre} counterparts. Expression of NKRs are similar except for NKG2D that was less expressed in *Cish*$^{fl/fl}$*Ncr1*^{iCre} NK cells. Indeed, CD122 is more expressed as previously described (online supplemental figure 3C–F). *Cish*$^{fl/fl}$*Ncr1*^{iCre} and *Cish*$^{+/+}$*Ncr1* ^{iCre} NK cells from LAK cultures were stimulated with plate bound NKp46, NK1.1 or NKG2D antibodies. Primed *Cish*$^{fl/fl}$*Ncr1*^{iCre} NK cells showed more expression of IFN-γ especially on NKp46 and NKG2D stimulations (figure 4D), no difference was detected with PMA/ionomycin (online supplemental figure 3G). On short NKp46, NK1.1 or NKG2D cross-linking stimulations, ERK phosphorylation

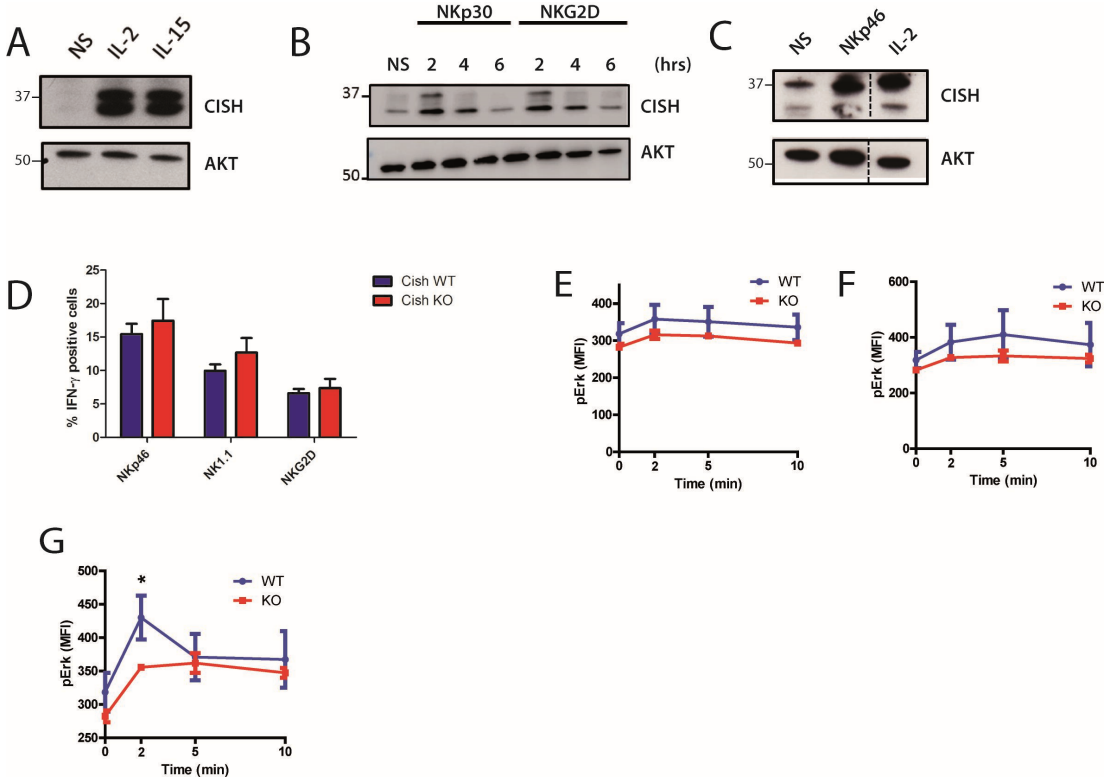

Figure 3 CISH is expressed on natural cytotoxicity receptors stimulation but have a moderate role in naïve NK cells. (A, B) Human KHYG-1 NK were stimulated for 4 hours with IL-2 (3000 UI/mL) and IL-15 (50 ng/mL) (A), NK-92 cells stimulated with coated anti-NKp30 or anti-NKG2D antibody (2 µg/mL) for the indicated time (B). Cell lysates were analyzed by immunoblotting for CISH or AKT (loading control). (C) Spleen purified NK cells were stimulated for 4 hours with IL-2 (3000 UI/mL) or coated anti-NKp46 antibody. Cell lysates were analyzed by immunoblotting for CISH or Akt (loading control). (D–G) Total splenic cells were harvested from 6 to 8 week-old *Cish*$^{+/+}$ and *Cish*$^{-/-}$ mice and depleted of red blood cells. (D, E) Cells were cross-linked with anti-NK1.1, NKp46 and NKG2D coated antibodies for 4 hours. FACS analysis of IFN-γ production (D) was assessed. (E–G) Cells were cross-linked with coated anti-NK1.1, NKp46 and NKG2D for 2, 5 and 10 min. Flow cytometric analysis of ERK1/2 phosphorylation status in NK cells was assessed. (D) Mean±SE of cells from five different mice and independent experiments. (E–G) Mean±SE of cells from three different mice and two independent experiments. *p <0.05,(Student's t-test). CISH, cytokine inducible SH2-containing protein; NK, natural killer.

increases in *Cish*$^{fl/fl}$*Ncr1*^{iCre} NK compared with *Cish*$^{+/+}$*Ncr1*^{iCre} (figure 4E–G), this was also detected with PMA/ionomycin (online supplemental figure 3H). Since LAK cells have been activated with IL-2 and CISH is known to be cytokine-inducible (figure 3A), they express more CISH thus increasing the functional difference on NKRs stimulation compared with naïve NK cells (figure 3D–G).

Specific deletion of CISH in NK cells enhances immunity to metastasis

We next tested whether CISH deletion in NK cells confers enhanced tumor immunity *in vitro* and *in vivo*. *In vitro* coculture of B16F10 melanoma cells with CISH KO NK cells led to an increased apoptosis compared with WT NK cells (figure 5A). Then, intravenous administration of B16F10 showed a decrease in metastatic nodules in the lung of *Cish*$^{fl/fl}$*Ncr1*^{iCre}compared with *Cish*$^{+/+}$*Ncr1*^{iCre} controls(figure 5B). Similarly, *in vitro* coculture of E0771 breast cancer cells with CISH KO NK cells led to an increased apoptosis compared with WT NK cells (figure 5C). Then E0771-GFP/Luc cells were administered and tumor burden was significantly reduced at day 7 and 14 in *Cish*$^{fl/fl}$*Ncr1*^{iCre} mice, reduction in lung and liver mestastasis was also observed (figure 5E–G).

Specific deletion of CISH in mature NK cells enhances immunity to primary tumors

Remarkably, we found that the growth of orthotopic E0771 tumor implanted in the mammary fat pad was also significantly reduced in *Cish*$^{fl/fl}$*Ncr1*^{iCre} mice compared with *Cish*$^{+/+}$*Ncr1*^{iCre} mice (figure 6A,B). This coincided with reduced spontaneous metastasis to the lungs (figure 6C,D). We also found more absolute number of infiltrated NK cells in the tumor (figure 6E). No difference of expression in activation markers CD69/CD25 or in NK cells subtypes (KLRG1, CD11b) in tumor-infiltrated CISH KO NK cells vs WT cells was detected (online supplemental figure 4A–D). However, we found a higher expression of CD122 (IL15-Rβ) receptor at the surface of CISH KO NK cells compared with WT cells (figure 6F), in accordance with the in vitro observations (figure 2D).

One of the main causes of relapse in immunotherapy treatment is the exhaustion of cytotoxic cells due to inhibiting receptor expression. We thus tested for expression of

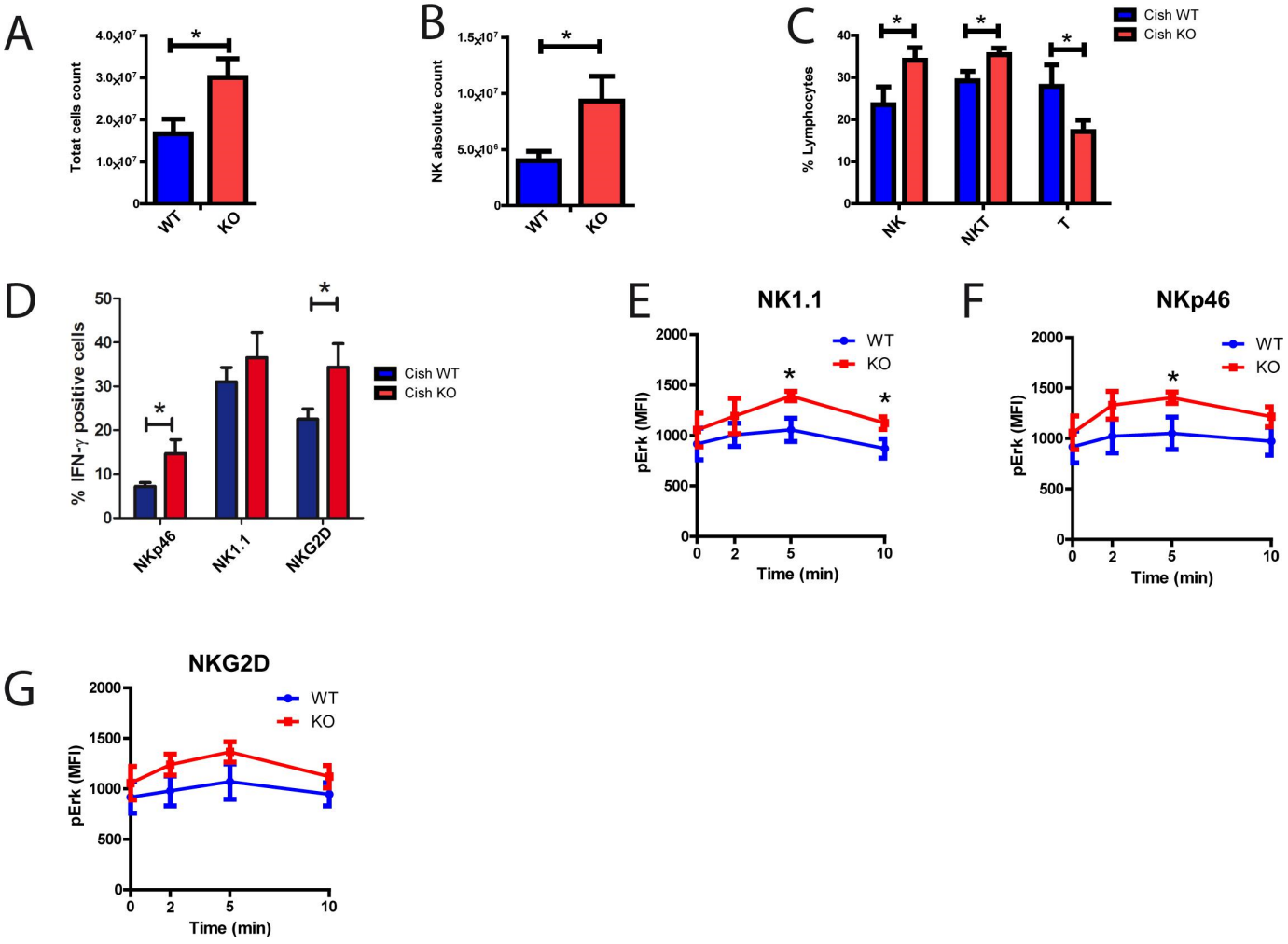

Figure 4 Cish deletion favors ex vivo expanded NK cells proliferation, functions and signaling. (A–G) Total splenocytes were expanded in IL-2 (1000UI/mL). (A) Histograms showing absolute numbers of cells that have proliferated at day 6. (B) NK cells gated by FACS (NK1.1+, CD3-) absolute count. (C) FACS gated histogram percentage of NK cells (NK1.1+, CD3-), NKT cells (NK1.1+, CD3+) and T cells (NK1.1-, CD3+). (D–F) After an overnight IL-2-starvation, cells were stimulated with anti-NK1.1, NKp46 or NKG2D coated antibodies for 4 hours. FACS analysis of NK cells and their IFN-γ production (D) was assessed. (E–G) Cells were cross-linked with anti-NK1.1, anti-NKp46 and anti-NKG2D coated antibodies for 2, 5 and 10 min. Flow cytometric analysis of ERK1/2 phosphorylation in NK cells was assessed. (A–D) Mean±SE of 5 different mice and independent experiments. (E–G) Mean±SE of 3 different mice and two independent experiments. *p <0.05,(Student's t-test). MFI, mean fluorescence intensity; NK, natural killer

the PD-1, TIM-3 and T-cell immunoreceptor with Ig and ITIM domains (TIGIT) receptors that are all suggested to be a part of NK cell exhaustion[20] (figure 6G). Interestingly, only TIGIT expression was strongly decreased in infiltrated CISH KO NK cells compared with WT NK cells (figure 6H–J). We next used previously published Database of Single cells mapping of immune cells infiltrated in human breast tumors.[21] Interestingly, in infiltrated NK cells, *TIGIT* is one of the top ten up-regulated gene in presence of *CISH* (online supplemental figure S4E) and expression was greatly reduced when *CISH* gene is absent (online supplemental figure 4F). This latter result suggests that *TIGIT* and *CISH* are regulated similarly in NK cells. These data highlight a previously unappreciated role for NK cells in controlling the growth of primary tumors in addition to metastatic cancer cells.

Targeting *CISH* genetically in human NK cells using CRISPR(i)-Cas9 technology improves their function

The use of human NK cells in adoptive transfer therapy has showed promising results.[22] Using the cutting edge tool CRISPR(i)-dCas9 we decided to target *CISH* in human NK-92 cell line.[23] This method represses gene-targeted promoter and reduce drastically potent 'off-target' effect. NK-92 cells were transduced with a KRAB-dCAS9-mCherry and a control or *CISH* sgRNA-GFP (figure 7A). mCherry and GFP double positive cells were selected by cell sorting. CISH expression is reduced in sgCISH transduced cells compared with control NK-92 transduced cells (figure 7B). In a co-culture assay, sgCISH NK-92 cells led to an increased apoptosis of K562 target cells compared with control transduced NK-92 cells (figure 7C). Similarly, sgCISH NK-92 cells show higher level of degranulation

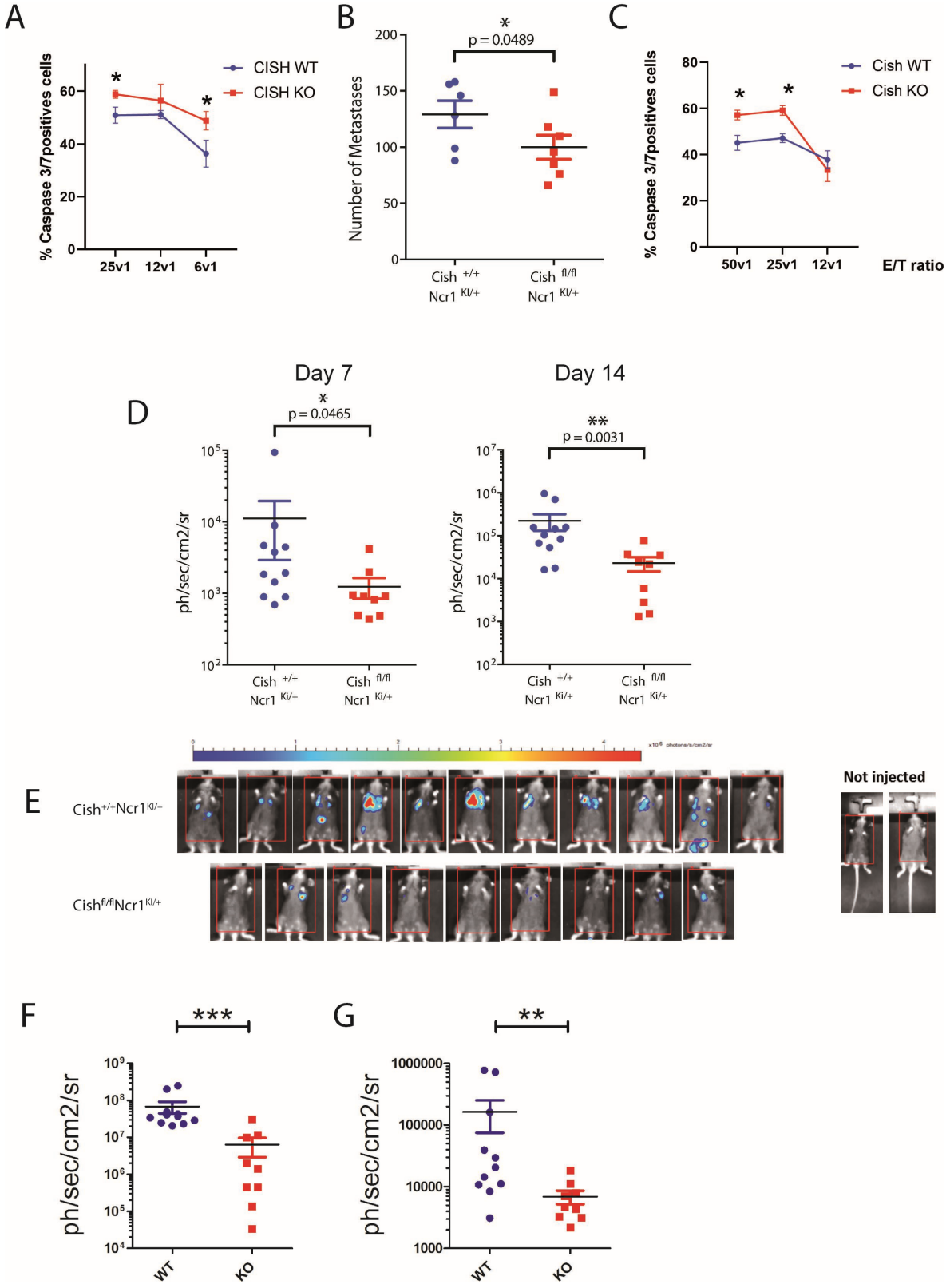

Figure 5 Specific deletion of CISH in NK cells enhances immunity to metastasis. (A) B16F10 cells positive for caspase 3/7 by FACS cocultured with LAK WT or KO cells (B) 3×10^5 B16F10 melanoma cells were injected i.v. into *Cish* $^{+/+}$*Ncr1*$^{Ki/+}$ and *Cish* $^{fl/fl}$*Ncr1*$^{Ki/+}$ mice and 14 days later lung metastases were enumerated. (C) E0771 cells positive for caspase 3/7 by FACS cocultured with LAK WT or KO cells (D–G) 5×10^5 EO771-GFP$^+$ Luciferase$^+$ breast cancer cells were injected i.v. into *Cish* $^{+/+}$*Ncr1*$^{Ki/+}$ and *Cish* $^{fl/fl}$*Ncr1*$^{Ki/+}$ mice and metastatic burden was quantified by luminescence at day 7 and 14. (C) Representative luminescence pictures are showed. (D, E) Spontaneous metastatic burden was quantified by luminescence at day 14 in the lung (D) and liver (E). *P≤0.05 **p≤0.01 ***p≤0.001 (unpaired Student's t-test). (B) Mean±SE of n≥6 different mice per group. (D–G) Mean±SE of n≥9 different mice per group. CISH, cytokine inducible SH2-containing protein; NK, natural killer; i.v, intravenous.

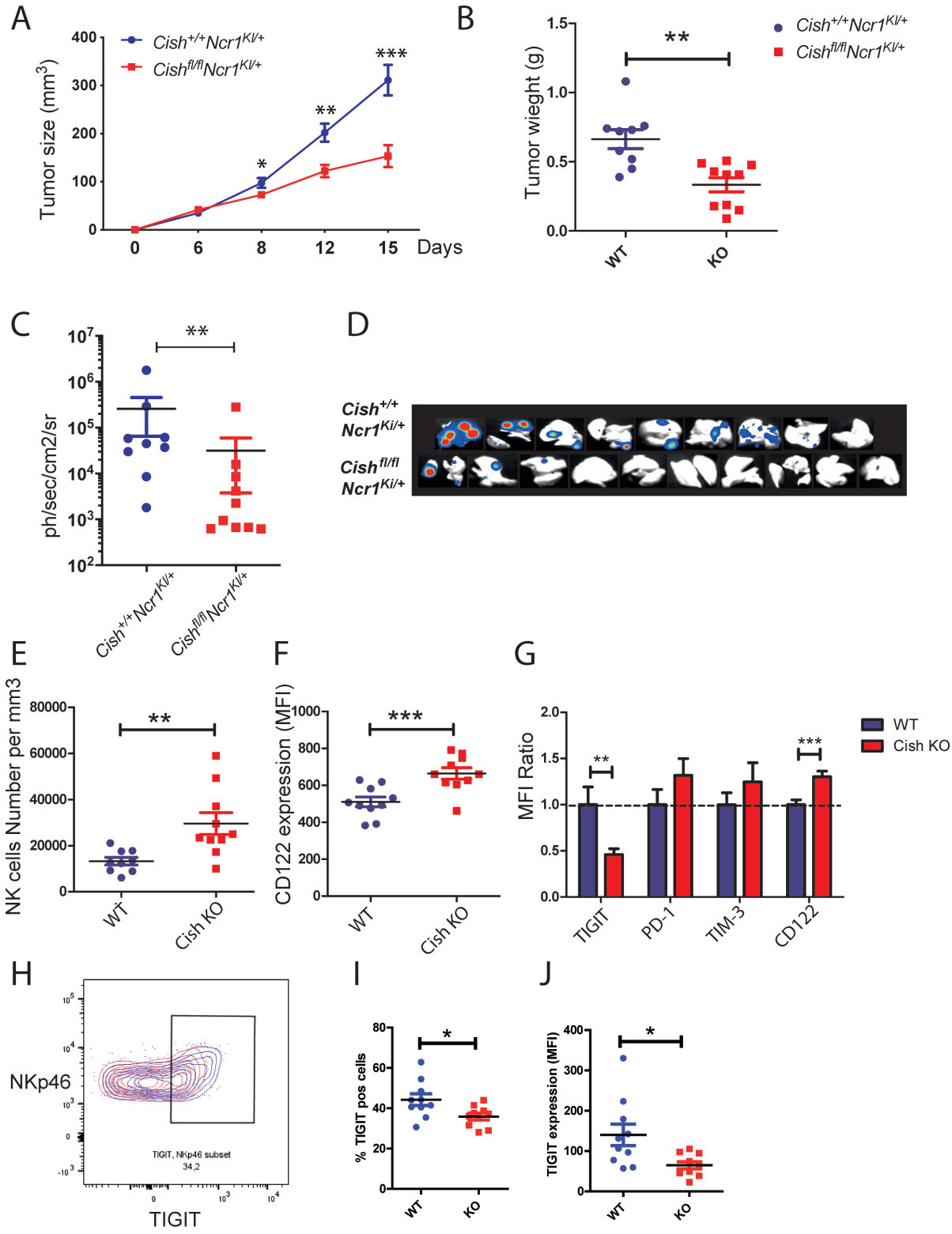

Figure 6 Specific deletion of CISH in mature NK cells enhances immunity to primary tumors (A–J) Orthotopic injection of EO771-GFP$^+$ Luciferase$^+$ breast cancer cells in the mammary fat pad of *Cish* $^{+/+}$*Ncr1*$^{Ki/+}$ and *Cish*$^{fl/fl}$*Ncr1*$^{Ki/+}$ mice. (A) Measure of tumor growth in mm^3 at indicated timepoints. (B) Measure of tumor weight at day 15. (C, D) At day 15, lungs from tumor bearing *Cish* $^{+/+}$*Ncr1*$^{Ki/+}$ and *Cish*$^{fl/fl}$*Ncr1*$^{Ki/+}$ mice were analyzed and metastatic burden quantified by luminescence. (D) Pictures of lung luminescence. (E) Numbers of infiltrated NK cells (NK1.1$^+$, CD3$^-$) /mm^3 of tumors. (F) Mean fluorescence of CD122 on Infiltrated NK cells. (G) FACS was used to quantify the MFI ratio of TIGIT, PD-1, TIM-3 and CD122 to WT infiltrated NK cells. (H–J) TIGIT expression analysis by FACS. (H) Representative plot comparing *Cish* $^{+/+}$*Ncr1*$^{Ki/+}$ and *Cish*$^{fl/fl}$*Ncr1*$^{Ki/+}$ TIGIT profile. (I) Percentage of TIGIT positive cells and (J) MFI of TIGIT. Mean±SE of n≥9 different mice per group; *p <0.05, **p<0.01, ***p<0.01 (Student's t-test). CISH, cytokine inducible SH2-containing protein; MFI, mean fluorescence intensity; NK, natural killer; TIGIT,T-cell Immunoreceptor with Ig and ITIM domains.

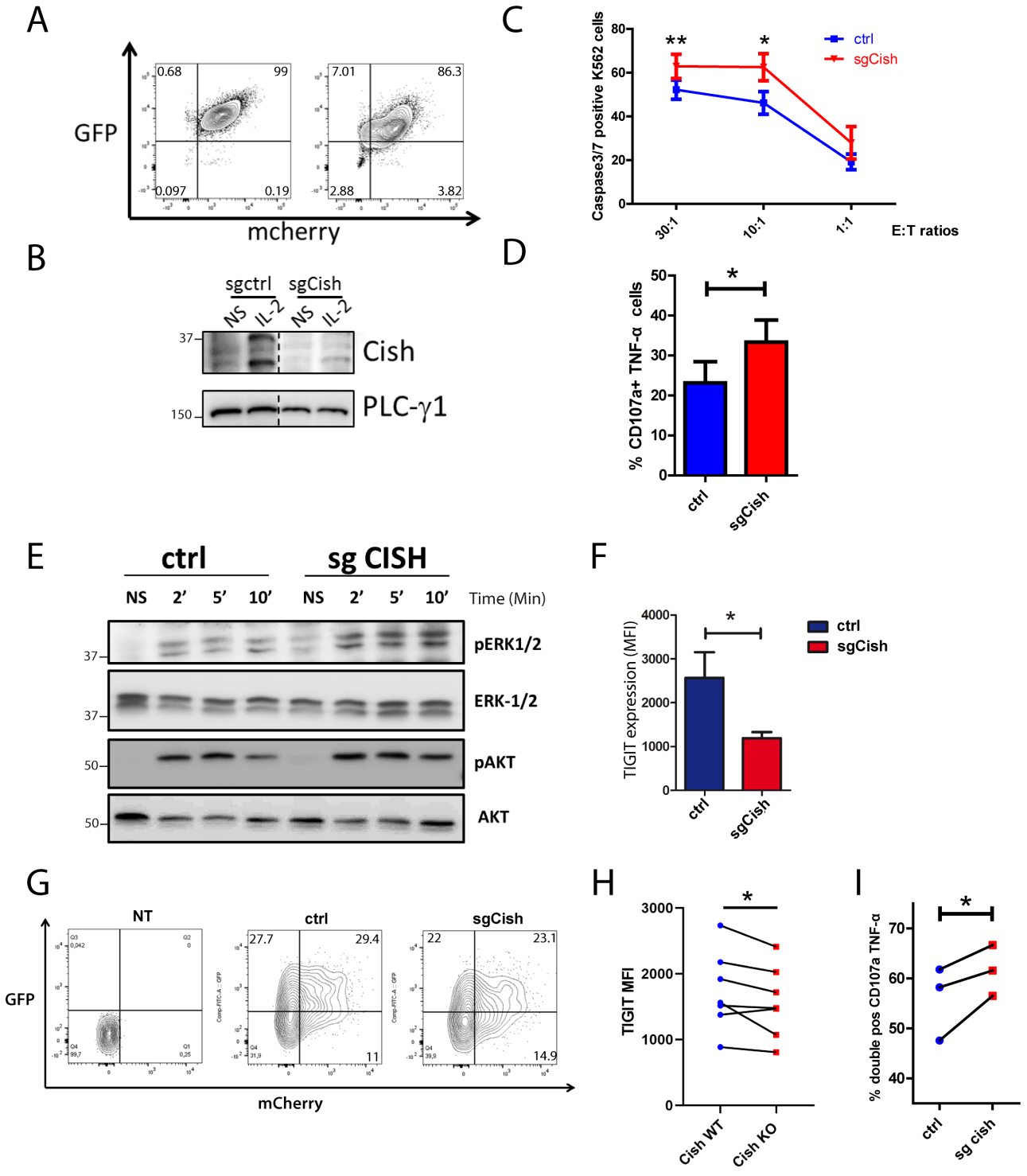

Figure 7 NK-92/primary NK cells were transduced with a KRAB-dCAS9 construct coexpressing mCherry and a ctrl or Cish SgRNA construct coexpressing GFP. (A) Validation of constructs expression by flow cytometry in NK-92 cells. (B) Validation of CISH silencing by western blot, following IL-2 stimulation for 4 hours. (C, D) 4 hours coculture of NK-92 WT or KO cells with K562 cancer cells. (C) Cytotoxicity tests, K562 cells positive for caspase 3/7 marker are identified by FACS. (D) Percentage of NK-92 cells double positive for CD107a and TNF-α identified by flow cytometry. (E) On an overnight IL-2 starvation, cells were stimulated with biotinylated NKp30 antibody (10 µg/mL) then cross-linked with streptavidin (20 µg/mL). Cell lysates were analyzed by immunoblotting for p(T202/Y204)-ERK-1/2, ERK-1/2, p(S473)-AKT or AKT. (F) TIGIT expression was assessed by flow cytometry comparing NK-92 control (ctrl sg) and CISH-KO NK-92 (Sg CISH). (G) Validation of constructs expression by flow cytometry in primary NK cells 2 days after transduction. (H) Flow cytometric analysis of primary NK transduced with construct ctrl or sgCISH. MFI expression of TIGIT(I) 4 hours cocculture assay of sgCISH or control transduced primary NK cells with K562 cancer cells at a ratio of 1:30 effector:target (E:T). Percentage of double positive cells for CD107a and TNF-α was identified by flow cytometry. *p <0.05, **p<0.01 (Student's t-test). CISH, cytokine inducible SH2-containing protein; MFI, mean fluorescence intensity; NK, natural killer; TIGIT,T-cell Immunoreceptor with Ig and ITIM domains.

(CD107a+) and production of TNF-α compared with control transduced NK-92 cells (figure 7D). We showed previously that CISH is expressed on NKp30 stimulation in NK-92 cells. Control and sgCISH transduced cells were stimulated with cross-linked NKp30 antibody during indicated time (figure 7E). WB analyses were performed showing an increase of ERK-1/2 and AKT phosphorylation in cells transduced with sgCISH compared with control. This difference is not due to NKp30 expression difference (online supplemental figure S5B). We also checked for TIGIT expression in these genetically modified cells and observed less TIGIT expression when CISH is downregulated (figure 7F). SgCISH NK-92 were more potent to kill *in vitro* and decrease the number of U937 lymphoma cells *in vivo* in an adoptive transfer experiment compared with control transduced NK-92 cells (online supplemental figure 5F–H).

Development of immunotherapies targeting primary NK cells has been limited in part due to their resistance to traditional viral gene delivery systems. Indeed, in NK-92 experiments using classical lentiviral vectors pseudotyped with the Vesicular stomatitis virus G envelope we achieved only low transduction efficiency. In order to overcome this poor transduction efficiency we decided to use the endogenous baboon retroviral envelope for pseudotyping of the lentiviral vectors that showed recently impressive results for primary NK cells transduction.[17] Using a MOI of 2, around 50% of transduction efficiency was achieved for KRAB-dCAS9-mCherry,ctrl or *CISH* sgRNA-GFP and 20%–30% of double positive cells (figure 7G). Expression of surface of TIGIT was again lower in cells transduced with sgCISH compared with control Transduced cells (figure 7H) but without affecting receptors NKp30, NKG2D or CD122 (online supplemental figure 5G–J). After sorting double positive cells, coculture assay with K562 cells (figure 7H) showed that primary NK cells transduced with sgCISH express more CD107a and TNF-α compared with control transduced cells.

Altogether, we showed the feasibility and importance to target CISH in human NK cells using a technology combining the CRISPR(i)-dCas9 tool with a new lentiviral pseudotype allowing high level transduction efficiency in primary NKs.

DISCUSSION

Many of the current treatments focus on targeting inhibitory cell surface receptors to improve cytotoxic lymphocyte antitumor function. Here, we suggest that targeting intracellular 'brakes' such as CISH may also be of beneficial interest.

Cish-deficient NK cells are terminally mature and develop normally. This, contrasting the maturation defect and DNAM-1 over expression that was found on germline CISH-deleted NK cells.[13] We believe that CISH regulates these receptors expression processes at an earlier NK cell stage prior to NKp46 expression. Indeed, targeting CISH using CRISPR-Cas9 technology in iPSCs-derived NK cells lead also to a delay in NK cell differentiation.[24] This suggests that targeting CISH in mature NK cells may be a safe strategy to use in clinic to prevent potential NK developmental defects.

Our gene set enrichment analysis shows upregulation of signaling pathways essential for NK cell activation and cycling. This observation indicates that in absence of CISH, NK cells are 'programmed' to proliferate actively and to be activated. This also suggesting that CISH may also be a part of signaling pathways other than cytokine signaling pathways. Indeed, our work highlight the involvement of CISH in NCR signaling, both in mice and human cells. Thus, like we previously showed in T cells[11] and here in NK cells, CISH is not only regulating cytokine receptor signaling but has a more complex role in cell signaling by being involved in negative feedback loops downstream of NKRs pathways.

In naïve NK cells, we only saw a mild effect of CISH-absence functionally. We believe this is due to the fact that CISH is expressed at a very low level at steady state but will be expressed on cytokine and/or NCR stimulations. This explains the greater activation of our CISH KO NK cells compared with WT cells in LAKs cells. Activating receptors were stimulated sequentially here, but *in vivo* NK cell responses to infectious or tumor cells depend on the balance between several activating and inhibitory signals. Thus, the increased NK cells killing properties observed in absence of CISH is probably the addition of several overactivated signaling pathways.

It was previously shown that CISH is a potent checkpoint in NK cell-mediated anti-metastatic effect using a CISH germline deficient mouse *Cish*$^{-/-}$.[12] However, CISH deletion in DC,[25] macrophages[26] and T cells[11 27] also favored the activation of these immune cells. This new conditional *Cish*-deficient mouse model univocally shows that he absence of CISH in NK cells is sufficient to decrease metastasis formation.

Previously, an orthotopic injection of E0771 breast cancer cells into germline *Cish*$^{-/-}$ mice resulted in decreased tumor burden and metastasis to other organs.[12] However, there is limited evidence to suggest that the decrease in tumor size is due to increased NK cell function alone, or the orchestration of multiple immune cells lacking CISH (such as CD8 +T cells). Strikingly, when *Cish*$^{fl/fl}$*Ncr1*^{iCre} mice were orthotopically implanted with E0771 breast cancer cells, conditional NK cells *Cish*-deletion was sufficient to decrease primary tumor growth and the subsequent spontaneous metastasis in the lung and liver.

We observed more NK cells infiltrated the tumor in absence of CISH. The reason to that might be multifactorial. One reason is that they are more sensitive to IL-15 and thus proliferate more efficiently in response to IL-15 present in the tumor microenvironment. We also show in here that activated NK cells in absence of CISH produce more cytokines and degranulate more, especially in response to NCR receptors that are essential for tumor recognition and killing. This means that these cells are more eager to recognize and to kill directly their targets but also probably to influence other immunes cells sucn as DCs and CD8^{+} T cells due to their

cytokine's secretion. Unexpectedly, we also observed that Cish KO NK cells express less TIGIT that WT cells. So far, TIGIT has been the only one well defined checkpoint inhibitor receptor involved in NK cell exhaustion.[28] This latter result indicates that Cish KO NK cells are less exhausted than their WT counterparts. Further studies are required to understand in detail if TIGIT and CISH are regulating each other's expressions or if they are regulated by the same signaling pathways, as it has been suggested for example for IL-15.[29]

NK cell immunotherapy holds great promise as an 'off-the-shelf' cell therapy but their full potential has not been reached yet. Here we propose to target these cells with the elegant CRISPR(i)-dCas9 tool and show its feasibility in primary NK cells using the appropriate endogenous baboon retroviral envelope. Other protocols have been proposed to target NK cells from blood using other viruses or electroporation methods.[30 31] But all these protocols are using the regular Cas9 construct cutting irreversibly the targeted gene. Here we show for the first time that repressing CISH transcription using dCas9-KRAB construct is sufficient to improve primary NK cells functions. This method not only prevents classical off-target effects, but also can be used reversibly to avoid potent undesired side effects.[23]

CONCLUSION

In conclusion, targeting CISH improves NK cell ex vivo proliferation, functions and signaling activation of several pathways such as cytokines and NCRs. *In vivo* CISH absence favors NK cell numbers to the tumor burden, optimize their killing properties and limit NK cell exhaustion. We finally propose a new method to efficiently target gene in primary human NK cells.

Thus, we further characterized the inhibition of CISH as a method to unleash the NK cell antitumor response. Releasing NK cell inhibition by targeting CISH is a safe strategy to improve NK cell antitumor properties and we support the clinical development of this approach.

Author affiliations
[1]Immunity and Cancer Team, Onco-Hemato Immuno-Onco Department, OHIO, Institut Paoli-Calmettes, Inserm, CNRS, Cancer Research Centre, CRCM, Marseille, France
[2]Immunology Program, Sloan-Kettering Institute, New York City, New York, USA
[3]INSERM, Unité 1111, Université Claude Bernard Lyon 1, Centre National de la Recherche Scientifique, Unité Mixte de Recherche (UMR) 5308, CIRI-International Center for Infectiology Research, Nice, France
[4]Innate Pharma Research Labs, Innate Pharma; Centre d'Immunologie de Marseille-Luminy, CIML; Service d'Immunologie, Marseille Immunopole, Hôpital de la Timone, Assistance Publique-Hôpitaux de Marseille, Aix Marseille Université, Inserm, CNRS, Marseille, France
[5]Department of Biochemistry and Molecular Biology, Biomedicine Discovery Institute, Monash University, Clayton, Victoria, Australia

Twitter Pierre-Louis Bernard @PL_Bernard, Jacques Nunes @NUNESJacques1 and Geoffrey Guittard @Geoffguittard

Contributors P-LB, SP, VL, AG, EJ, RC, JV and GG all performed experiments. GG, and JN designed experiments and analysed the data. RD, DO, EVi and NDH contributed intellectual input and helped to interpret data. GG and JN led the research program. NDH, GG and JN wrote the manuscript. GG and JN are responsible for the overall content as guarantor. All authors have reviewed and approved the submitted manuscript.

Funding This work is supported in France by institutional grants from the Institut National de la Santé et de la Recherche Médicale (Inserm), Centre National de la Recherche Scientifique (CNRS) and Aix-Marseille Université to CRCM; by project grants from the Fondation ARC pour la recherche sur le Cancer (PJA20161204835, PJA20191209406), Groupement des Entreprises Françaises dans la Lutte contre le Cancer (GEFLUC) Marseille-Provence, the Janssen Horizon Fonds de dotation and The fondation Bristol-Myers Squibb. P-LB and CCDS are supported by doctoral fellowships from Ligue Nationale contre le Cancer and VL by a doctoral fellowship from the Ministère de l'Education et la Recherche, then from the Fondation ARC pour la recherche sur le Cancer. GG was supported by a post-doctoral fellowship from the Fondation ARC pour la recherche sur le Cancer and is currently supported by the Janssen Horizon Fonds de dotation. DO is a Senior Scholar of the Institut Universitaire de France. We thank Cancéropôle PACA and the Plan Cancer Equipement (#17CQ047-00) for continued support the development of the TrGET preclinical assay platform. The team 'Immunity and Cancer' was labeled 'Equipe Fondation pour la Recherche Médicale (FRM) DEQ 20180339209' (for DO). Centre de recherche en Cancérologie de Marseille (Inserm U1068) and the Paoli Calmettes Institute are members of OPALE Carnot Institute, The Organization for Partnerships in Leukemia, Institut de Recherche Saint-Louis, Hôpital Saint-Louis, 75010 Paris, France. We wish to thank Bernard Malissen and Frédéric Fiore for their expertise to generate Tm1c Cishfl/fl mice (B6-Cishtm1cCiphe) at the Centre d'Immunophénomique (Ciphe) (Marseille, France), Esma Karkeni for participating in the characterization of the Cishfl/flNcr1Ki/+ mouse strain and Arnaud Capel for excellent animal husbandry. We are grateful to the staff of the CRCM animal facility for taking care of the mouse strain colonies and the CRCM cytometry platform for FACS analysis.

Competing interests EVi is an employee of Innate Pharma and has ownership and stock options. DO is cofounder and shareholder of Imcheck Therapeutics, Emergence Therapeutics, and Alderaan Biotechnology. NDH is a founder and shareholder of oNKo-Innate. NDH receives research funding from Servier, Paranta Biosciences and Anaxis Pharma. The remaining authors declare that the research was conducted in the absence of any commercial or financial relationships that could be construed as a potential conflict of interest.

Patient consent for publication Not applicable.

Provenance and peer review Not commissioned; externally peer reviewed.

Data availability statement Data are available on reasonable request.

ORCID iDs
Rebecca Delconte http://orcid.org/0000-0002-3066-4014
Vladimir Laletin http://orcid.org/0000-0003-3960-4218
Rémy Castellano http://orcid.org/0000-0002-0152-985X
Julien Vernerey http://orcid.org/0000-0002-5413-4210
Raynier Devillier http://orcid.org/0000-0002-4045-8310
Daniel Olive http://orcid.org/0000-0003-1299-4113
Els Verhoeyen http://orcid.org/0000-0001-9224-5491
Eric Vivier http://orcid.org/0000-0001-7022-8287
Nicholas D Huntington http://orcid.org/0000-0002-5267-7211
Jacques Nunes http://orcid.org/0000-0003-4865-0400
Geoffrey Guittard http://orcid.org/0000-0002-6061-8553

REFERENCES

1 Shimasaki N, Jain A, Campana D. NK cells for cancer immunotherapy. *Nat Rev Drug Discov* 2020;19:200–18.
2 Sun H, Sun C. The rise of NK cell checkpoints as promising therapeutic targets in cancer immunotherapy. *Front Immunol* 2019;10:2354.
3 Huntington ND, Cursons J, Rautela J. The cancer-natural killer cell immunity cycle. *Nat Rev Cancer* 2020;20:437–54.
4 Gasteiger G, Rudensky AY. Interactions between innate and adaptive lymphocytes. *Nat Rev Immunol* 2014;14:631–9.
5 Liu E, Marin D, Banerjee P, *et al*. Use of CAR-transduced natural killer cells in CD19-positive lymphoid tumors. *N Engl J Med* 2020;382:545–53.
6 Chockley PJ, Chen J, Chen G, *et al*. Epithelial-mesenchymal transition leads to NK cell-mediated metastasis-specific immunosurveillance in lung cancer. *J Clin Invest* 2018;128:1384–96.
7 Sathe P, Delconte RB, Souza-Fonseca-Guimaraes F, *et al*. Innate immunodeficiency following genetic ablation of MCL1 in natural killer cells. *Nat Commun* 2014;5:4539.
8 Pasero C, Gravis G, Granjeaud S, *et al*. Highly effective NK cells are associated with good prognosis in patients with metastatic prostate cancer. *Oncotarget* 2015;6:14360–73.
9 Souza-Fonseca-Guimaraes F. NK cell-based immunotherapies: awakening the innate anti-cancer response. *Discov Med* 2016;21:197–203.
10 Guittard G, Dios-Esponera A, Palmer DC, *et al*. The Cish SH2 domain is essential for PLC-γ1 regulation in TCR stimulated $CD8^+$ T cells. *Sci Rep* 2018;8:5336.
11 Palmer DC, Guittard GC, Franco Z, *et al*. Cish actively silences TCR signaling in CD8+ T cells to maintain tumor tolerance. *J Exp Med* 2015;212:2095–113.
12 Delconte RB, Kolesnik TB, Dagley LF, *et al*. CIS is a potent checkpoint in NK cell-mediated tumor immunity. *Nat Immunol* 2016;17:816–24.
13 Delconte RB, Guittard G, Goh W, *et al*. NK cell priming from endogenous homeostatic signals is modulated by CIS. *Front Immunol* 2020;11:75.
14 Narni-Mancinelli E, Chaix J, Fenis A, *et al*. Fate mapping analysis of lymphoid cells expressing the NKp46 cell surface receptor. *Proc Natl Acad Sci U S A* 2011;108:18324–9.
15 Neri S, Mariani E, Meneghetti A, *et al*. Calcein-acetyoxymethyl cytotoxicity assay: standardization of a method allowing additional analyses on recovered effector cells and supernatants. *Clin Diagn Lab Immunol* 2001;8:1131–5.
16 Karkeni E, Morin SO, Bou Tayeh B, *et al*. Vitamin D controls tumor growth and CD8+ T cell infiltration in breast cancer. *Front Immunol* 2019;10:1307.
17 Colamartino ABL, Lemieux W, Bifsha P, *et al*. Efficient and robust NK-cell transduction with baboon envelope pseudotyped lentivector. *Front Immunol* 2019;10:2873.
18 Pegram HJ, Andrews DM, Smyth MJ, *et al*. Activating and inhibitory receptors of natural killer cells. *Immunol Cell Biol* 2011;89:216–24.
19 Viant C, Fenis A, Chicanne G, *et al*. SHP-1-mediated inhibitory signals promote responsiveness and anti-tumour functions of natural killer cells. *Nat Commun* 2014;5:5108.
20 Foroutan M, Molania R, Pfefferle A, *et al*. The ratio of exhausted to resident infiltrating lymphocytes is prognostic for colorectal cancer patient outcome. *Cancer Immunol Res* 2021;9:1125–40.
21 Azizi E, Carr AJ, Plitas G, *et al*. Single-cell map of diverse immune phenotypes in the breast tumor microenvironment. *Cell* 2018;174:e36:1293–308.
22 Guillerey C, Huntington ND, Smyth MJ. Targeting natural killer cells in cancer immunotherapy. *Nat Immunol* 2016;17:1025–36.
23 Gilbert LA, Horlbeck MA, Adamson B, *et al*. Genome-scale CRISPR-mediated control of gene repression and activation. *Cell* 2014;159:647–61.
24 Zhu H, Blum RH, Bernareggi D, *et al*. Metabolic reprograming via deletion of CISH in human iPSC-derived NK cells promotes in vivo persistence and enhances anti-tumor activity. *Cell Stem Cell* 2020;27:224–37.
25 Miah MA, Yoon C-H, Kim J, *et al*. CISH is induced during DC development and regulates DC-mediated CTL activation. *Eur J Immunol* 2012;42:58–68.
26 Queval CJ, Song O-R, Carralot J-P, *et al*. Mycobacterium tuberculosis controls phagosomal acidification by targeting CISH-mediated signaling. *Cell Rep* 2017;20:3188–98.
27 Yang XO, Zhang H, Kim B-S, *et al*. The signaling suppressor CIS controls proallergic T cell development and allergic airway inflammation. *Nat Immunol* 2013;14:732–40.
28 Zhang Q, Bi J, Zheng X, *et al*. Blockade of the checkpoint receptor TIGIT prevents NK cell exhaustion and elicits potent anti-tumor immunity. *Nat Immunol* 2018;19:723–32.
29 Villarino AV, Sciumè G, Davis FP, *et al*. Subset- and tissue-defined STAT5 thresholds control homeostasis and function of innate lymphoid cells. *J Exp Med* 2017;214:2999–3014.
30 Rautela J, Surgenor E, Huntington ND. Drug target validation in primary human natural killer cells using CRISPR RNP. *J Leukoc Biol* 2020;108:1397–408.
31 Pomeroy EJ, Hunzeker JT, Kluesner MG, *et al*. A genetically engineered primary human natural killer cell platform for cancer immunotherapy. *Mol Ther* 2020;28:52–63.

Targeting CISH enhances natural cytotoxicity receptor signaling and reduces NK cell exhaustion to improve solid tumor immunity

Authors: Bernard, P-L. [1], Delconte, R. B. [2,7], Pastor, S. [1], Laletin, V. [1], Costa Da Silva, C. [1], Goubard, A. [4], Josselin, E. [4], Castellano, R. [4], Krug, A. [8], Vernerey, J. [5], Devillier R. [1], Olive, D. [1], Verhoeyen, E.[8, 9], Vivier, E. [6], Huntington, N. D. [2,3], Nunès, J. A. [1]* and Guittard, G. [1]*

*These authors contributed equally

Supplementary figures and legend:

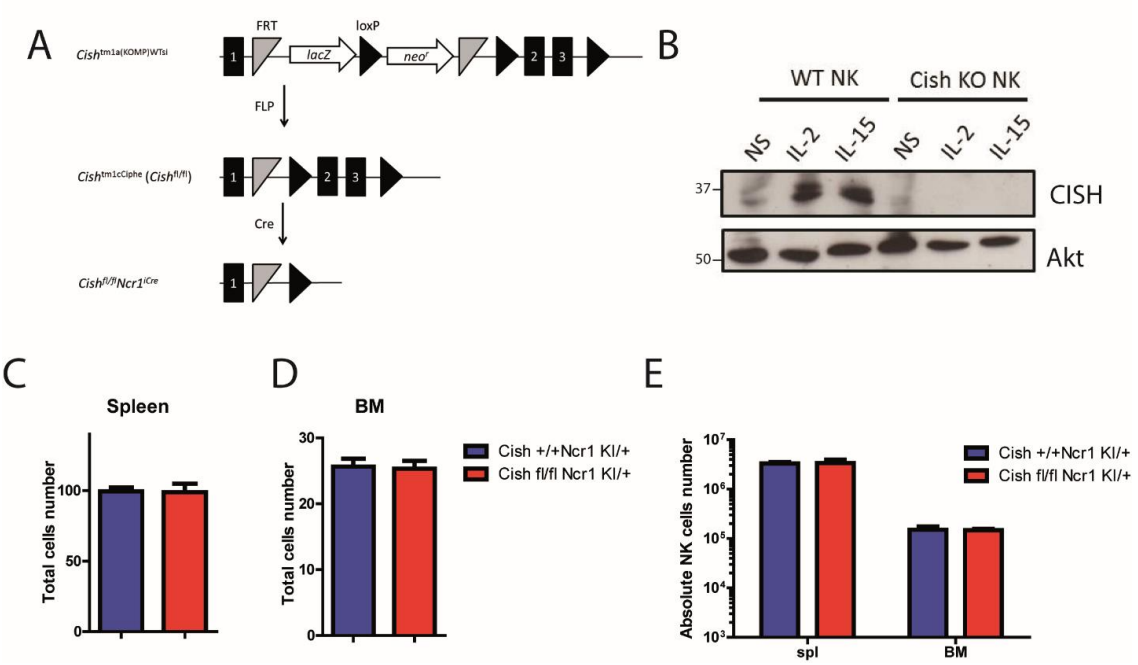

Supplemental figure 1 (**A**) Conditional *Cish*-deficient mice were generated by breeding mice containing the germline-transmitted Cish^{tm1a} allele to a FLP deleter strain to remove the *lacZ* and *neo^r* genes flanked by FRT recognition target sites. LoxP sites were inserted on either side of exons 2 and 3 to enable Cre-mediated inactivation of the Cish gene in

NK cells after breeding to Ncr1^{iCre} mice. (**B**) NK cells were purified from *Cish* $^{+/+}$*Ncr1*$^{Ki/+}$ or *Cish* $^{fl/fl}$*Ncr1*$^{Ki/+}$ spleens, expanded for 6 days with IL-15 and FACS sorted (NK1.1^{+}, NKp46^{+}, CD3^{-}, CD19^{-}). After overnight starvation, *Cish* $^{+/+}$*Ncr1*$^{Ki/+}$ and *Cish* $^{fl/fl}$*Ncr1*$^{Ki/+}$ NK cells were either untreated or stimulated for 4 hours with IL-2 or IL-15. Cell lysates were analysed by immunoblotting for Cish or Akt (loading control). (**C-D**) Total number of cells purified from *Cish* $^{+/+}$*Ncr1*$^{Ki/+}$ or *Cish* $^{fl/fl}$*Ncr1*$^{Ki/+}$ spleens (**C**) or Bone marrow (**D**). (**E**) Absolute number of NK cells (CD3-, NK1.1+) purified from *Cish* $^{+/+}$*Ncr1*$^{Ki/+}$ or *Cish* $^{fl/fl}$*Ncr1*$^{Ki/+}$ spleens or Bone marrow. (**C-E**) n=6 biological replicates mean ± s.e.m.

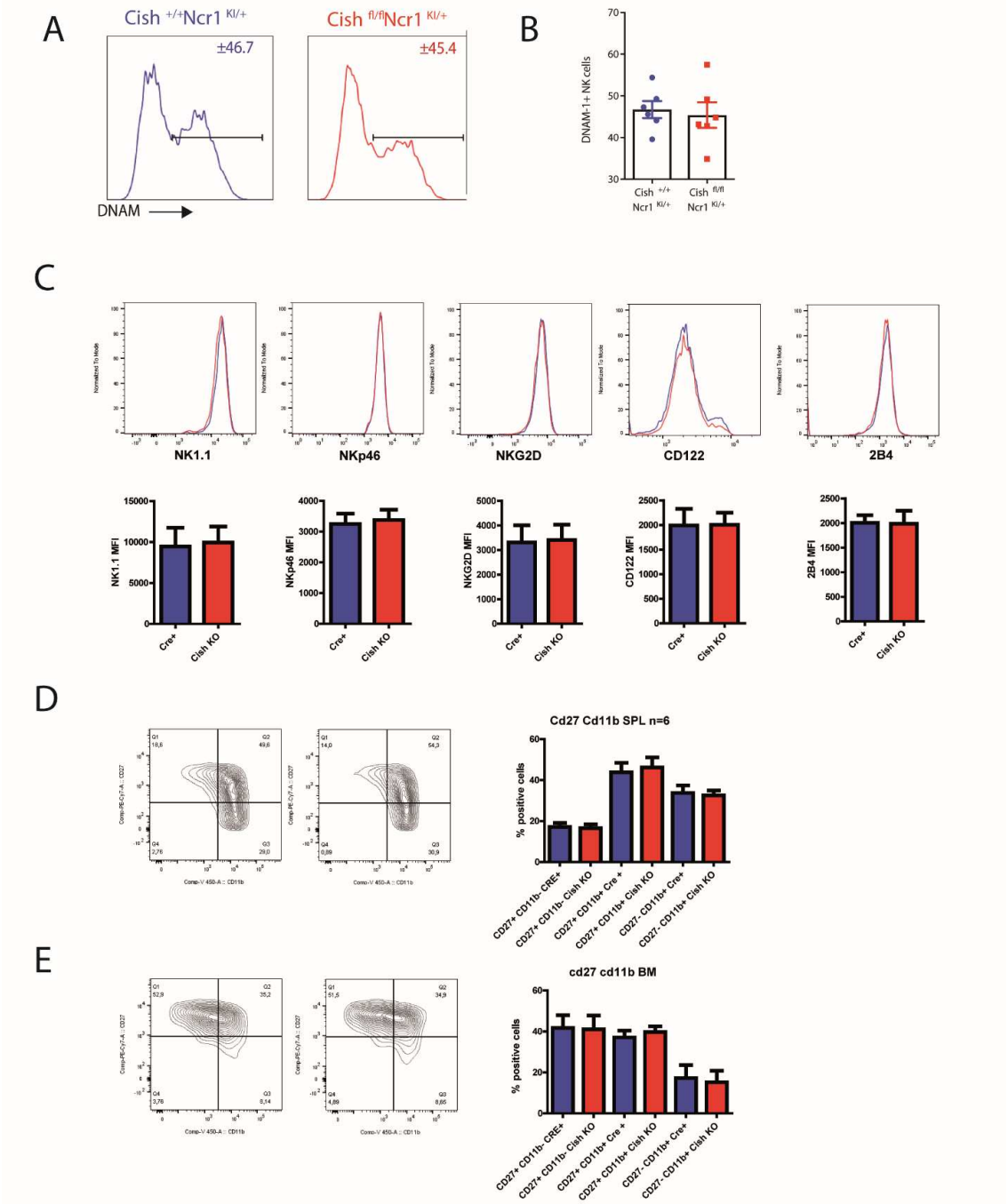
A
Cish +/+Ncr1 KI/+
±46.7
Cish fl/flNcr1 KI/+
±45.4
DNAM
B
DNAM-1+ NK cells
Cish +/+ Ncr1 KI/+
Cish fl/fl Ncr1 KI/+
C
NK1.1
NKp46
NKG2D
CD122
2B4
NK1.1 MFI
NKp46 MFI
NKG2D MFI
CD122 MFI
2B4 MFI
Cre+
Cish KO
D
Cd27 Cd11b SPL n=6
% positive cells
CD27+ CD11b- CRE+
CD27+ CD11b- Cish KO
CD27+ CD11b+ Cre +
CD27+ CD11b+ Cish KO
CD27- CD11b+ Cre+
CD27- CD11b+ Cish KO
E
cd27 cd11b BM
% positive cells

Supplemental figure 2. Splenic NK cells from *Cish* $^{+/+}$*Ncr1* $^{Ki/+}$ and *Cish* $^{fl/fl}$*Ncr1* $^{Ki/+}$ mice were phenotypically analysed by flow cytometry. (**A-B**) Frequency of DNAM-1^{+} NK cells and representative histogram is showed. (**C**) Representative histogram and Mean Fluorescence intensity (MFI) for NK1.1, NKp46, NKG2D, CD11 and 2B4 receptors are showed. (**D-E**) Frequency of CD27,Cd11b cells were measured within NK cell populations from the spleen, representative FACS plots and histograms are shown. n=6 biological replicates mean ± s.e.m.

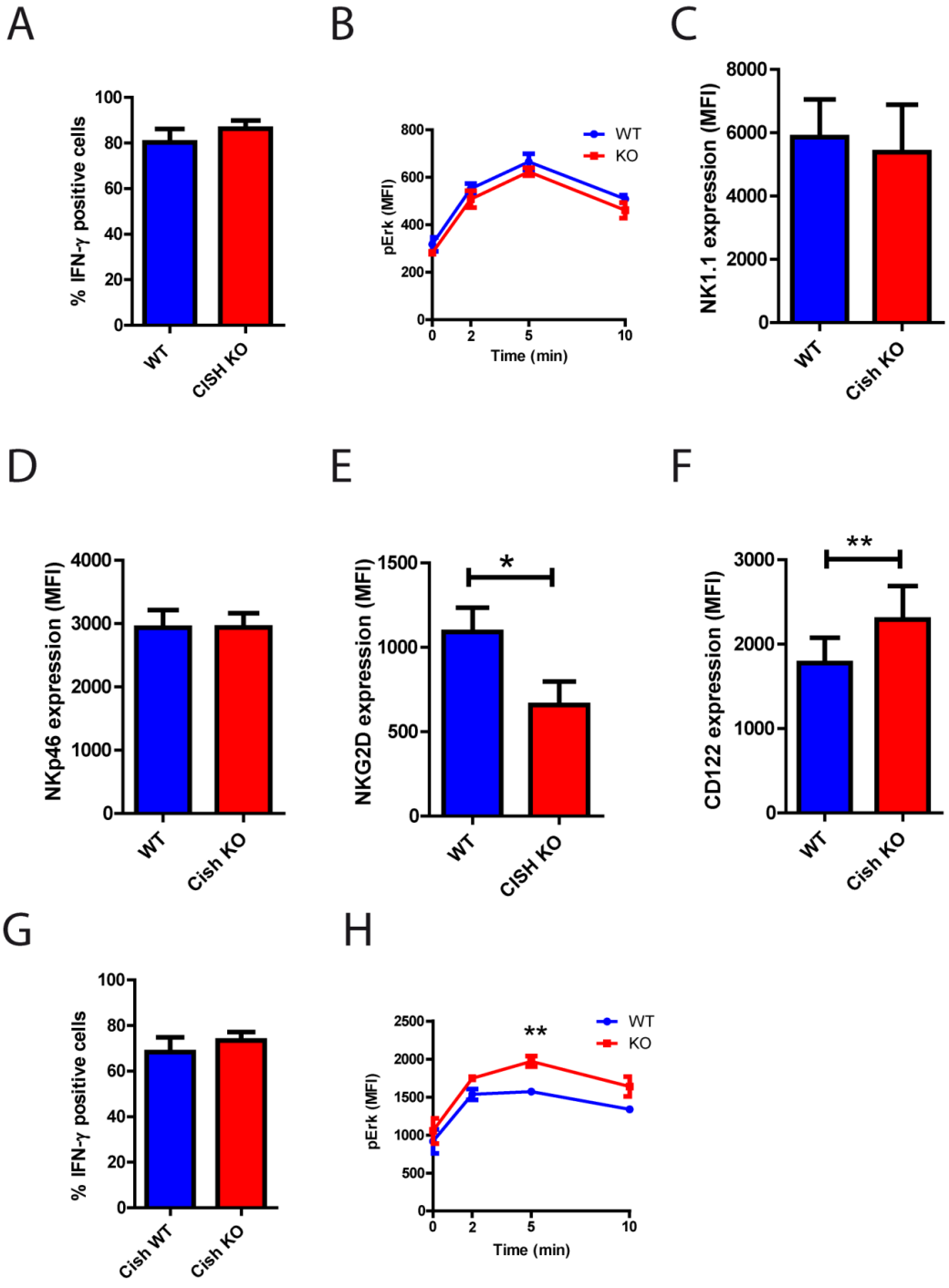

Supplemental figure 3. (**A**) splenocytes cells were stimulated with PMA and ionomycin

for 4 hrs. Flow cytometric analysis of NK cells and their IFN-γ production was assessed. (**B**) splenocytes cells were stimulated with PMA and ionomycin for 2, 5 and 10 minutes. Flow cytometric analysis of NK cells ERK1/2 phosphorylation was assessed. (**C-H**) Total splenocytes were expanded in IL-2 during 6 days (1000UI/ml), then an overnight IL-2-starvation was performed. (**C-F**) Flow cytometric analysis of NK cells and MFI expression of NK1.1 (**C**), NKp46 (**D**), NKG2D (**E**) and CD122 (**F**) receptors was assessed. (**G**) Expanded splenocytes (LAKs) were stimulated with PMA and ionomycin for 4 hrs. Flow cytometric analysis of NK cells and their IFN-γ production was assessed. (**H**) Expanded splenocytes (LAKs) were stimulated with PMA and ionomycin for 2, 5 and 10 minutes. Flow cytometric analysis of NK cells ERK1/2 phosphorylation was assessed. (**A-F**) n=4 biological replicates mean ± s.e.m. (**G-H**) n=3 biological replicates mean ± s.e.m. *$p<0.05$, **$p<0.01$ (Student's *t*-test).

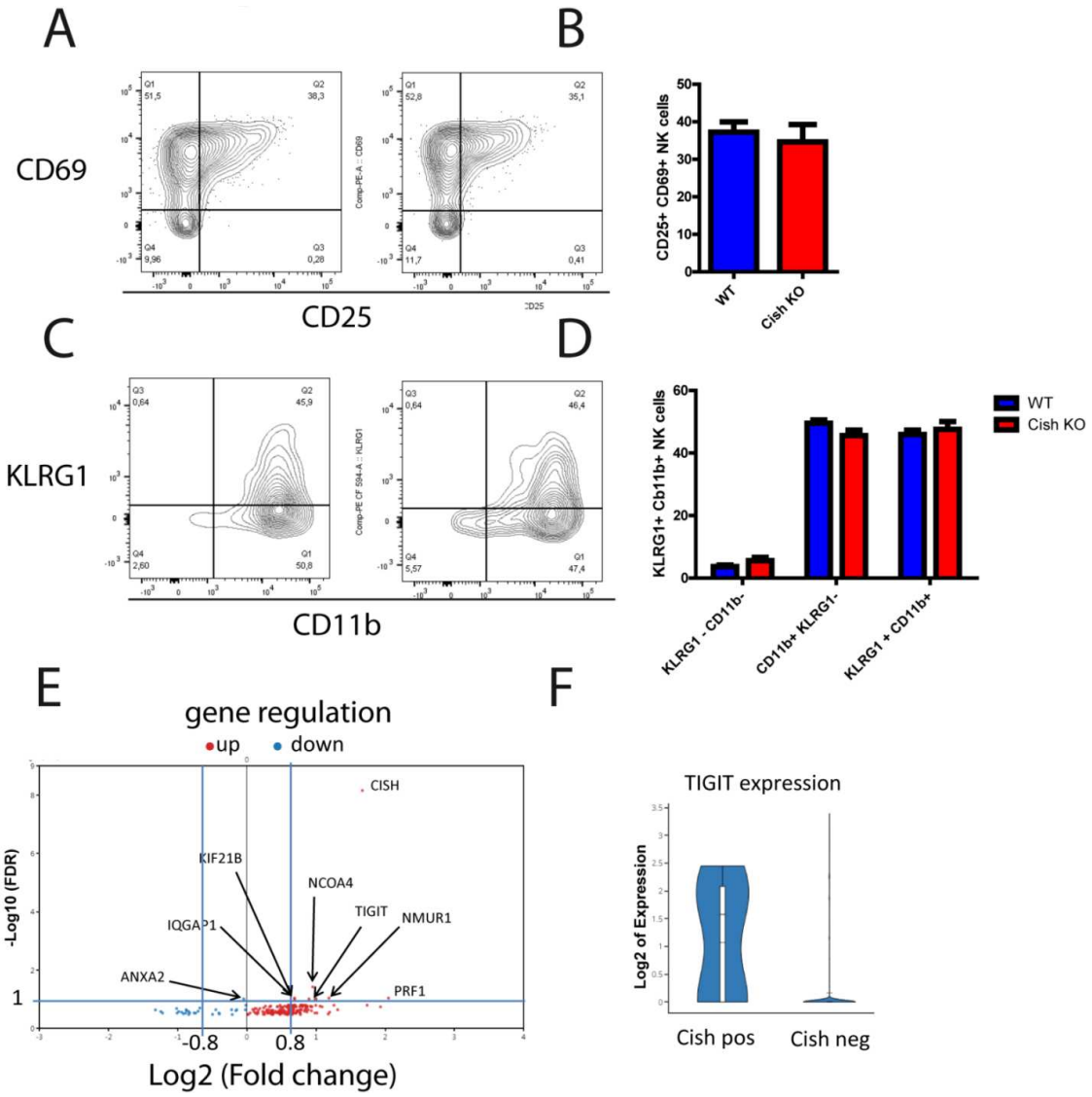

Supplemental figure 4. Orthotopic injection of EO771-GFP^{+} Luciferase^{+} breast cancer cells in the mammary fat pad of *Cish* $^{+/+}$*Ncr1*$^{Ki/+}$ and *Cish*$^{fl/fl}$*Ncr1*$^{Ki/+}$ mice. (**A-D**) Flow cytometry was used to quantify frequency of CD25 and CD69 cells (**A-B**) and KLRG1 and CD11b (**C-D**). (E-F). Loupe cell browser software was used to analyse previously published Database of Single cells mapping of immunes cells infiltrated in human breast tumors (Azizi et al., Cell 2018). We isolated infiltrated NK cells (*Cd3-*, *Ncam1+)* then

observed the expression of *Tigit* comparing *Cish+* NK cells with *Cish-* cells. (**E**) A volcano plot of significant (*-log10FDR>1*) differentially expressed genes with a log2fold change above 0.8 or below -0.8 was generated. y-axis is the negative log10 (FDR) value and x-axis is the log2-fold-change of the corresponding gene in $Cish^{-/-}$ vs $Cish^{+/+}$ comparison. Gene expression: blue = downregulated, red = upregulated. (**F**)Log2 expression of *Tigit* gene $Cish^{-/-}$ vs $Cish^{+/+}$ infiltrated NK cells.

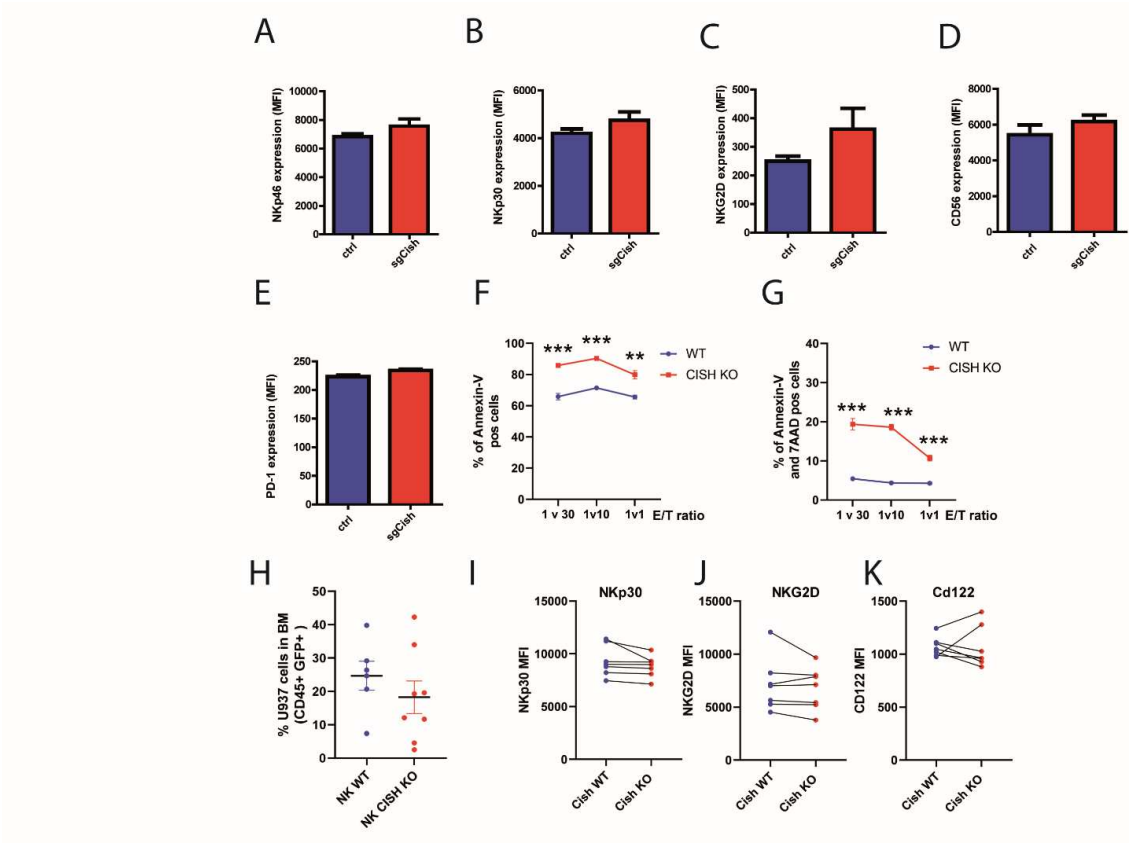

Supplemental figure 5. NK-92 / primary NK cells were transduced with a KRAB-dCAS9 construct co-expressing mcherry and a ctrl or Cish SgRNA construct co-expressing GFP. **(A-E)**. Flow cytometric analysis of NK-92 transduced with construct ctrl or sgCISH. MFI expression of NKp46 (**A**), NKp30 (**B**), NKG2D (**C**), CD56 (**D**) and PD-1 (**E**) receptors was assessed. (**F-G**) apopotosis (annexin V or late apoptosis 7AAD labeling) of U937 in co-culture with NK-92 transduced with construct ctrl or sgCISH in different Effector/target ratio is showed. (**H**) NSG female mice injected with U937 cells at day 0 and WT transduced or NK92 sgCISH NK-92 cells at days 1, 4, 8, 15 and 17. At Day 18 the number of U937 cells was evaluated by flow cytometry (U937 GFP+ cells). (**I-K**) Flow cytometric analysis

of primary NK transduced with construct ctrl or sgCISH. MFI expression of NKp30 (**I**), NKG2D (**J**) and CD122 (**K**) receptors was assessed.

Supplemental method :

Mice:

To generate Tm1c *Cish*$^{fl/fl}$ mice, sperm from *Cish*$^{tm1a(KOMP)WTsi}$ Knock-out mouse project repository (KOMP, UC Davis)[1] was injected into C57BL/6N host embryos at the Centre d'Immunophénomique (Ciphe) (Marseille, France). Homozygous *Cish*$^{tm1a(KOMP)WTsi}$ mice were then crossed with FLP-FRT mice to generate Tm1c *Cish*$^{fl/fl}$ mice (B6-Cish^{tm1cCiphe}). Then, Tm1c *Cish*$^{fl/fl}$ mice were crossed with *Ncr1*$^{iCre/+}$ mice [2]. Male and female mice were used between the ages of 6–12 weeks. Age and sex matched mice were used and cohort size was dictated by previous experience using these tumor models. Mice were bred and maintained under specific pathogen-free conditions at the Centre de Recherche en Cancérologie de Marseille (CRCM) animal facility. Animal experiments followed were performed in accordance with institutional committees and French and European guidelines for animal care.

Genotyping:

Tm1c *Cish*$^{fl/fl}$ genotyping was performed using the following PCR primers: *Cish* Tm1c Fwd, 5'-GAGGTCTCCCTGAGAACCCC-3'; *Cish* Tm1c Rev, Cis2, 5'-TTCCGCCACTGAGCCACATA-3'; with expected band sizes at 305 bp for WT alleles and 460 bp for floxed allele. *Ncr1*$^{iCre/+}$ genotyping was performed using the following PCR primers: iCRE Fwd, 5'-GGAACTGAAGGCAACTCCTG-3'; iCRE Fwd KI, 5'-GTCCATCCCTGAAATCATGC-3'; Rev WT:-5' TTCCCGGCAACATAAAATAAA-3'; with expected bands sizes at 300 bp for WT allele and 376 bp for KI allele.

Western blot :

Cells were lysed at 4 °C for 10 min in 1% NP-40 lysis buffer (50 mM Tris pH 7.4, 150 mM NaCl, 5 mM EDTA, protease inhibitor cocktail (Roche# 11836170001), 1 mM Na3VO4, 0.1% SDS). Samples were resolved by 10% SDS–polyacrylamide gel electrophoresis experiments. Blots were incubated overnight at 4 °C with the corresponding primary antibody directed CISH (Cell Signaling Technology #8731) or Akt (Cell Signaling Technology #9272) for Western blotting. Blots were incubated with horseradish peroxidase–conjugated secondary antibodies (Millipore) for 1 hr at room temperature. ECL (enhanced chemiluminescence; SuperSignal West Pico and SuperSignal West Femto, Pierce) was used to visualize protein bands.

NK cell cytotoxicity assays

Briefly, splenic NK cells were isolated and suspended in NK cell medium (phenol-red free RPMI 1640 containing 10% FCS, non-essential amino acids, L glutamine and sodium pyruvate, all from Gibco). The indicated target cells were labelled with 15µM Calcein-AM (Life Technologies) for 30 min at 37°C, washed twice and suspended in NK cell medium. Effector and target cells were combined at the indicated ratios in triplicate wells of a round-bottom 96 well plate and incubated at 37°C / 5% CO_2 for 4 hours. Calcein release was quantified by transferring 100 µL of cell-free supernatant to opaque 96 well plates and measuring fluorescent emission at the appropriate wave-length (excitation filter: 485±9 nm; cutoff: 515 nm; emission: 525±15 nm) using the EnVision Robot Plate Reader.

Enumeration of Apoptotic Cells:

The enumeration of apoptotic cells was performed using the CellEvent™ Caspase-3/7 Green Flow Cytometry Assay Kit (catalogue #: C10427; Thermo Fisher Scientific) following manufacturer's instructions.

Tumor cell lines:

B16F10 melanoma cells were obtained from ATCC and were maintained in Dulbecco's Eagle Modified Medium (DMEM) supplemented with 10% FBS. EO771 cell line was purchased from CH3 BioSystems LLC (Amherst, NY, USA). E0771-GFP^{+}-Luciferase were generated as was previously described [3] and were maintained in RPMI-1640 media supplemented with 10% FCS. NK-92 were obtained from ATCC were grown in RPMI-1640 (Invitrogen) medium supplemented with 1 mM sodium pyruvate, 100 U/ml penicillin, 100 µg/ml streptomycin and 20% heat-inactivated FCS plus 500 UI of IL-2. The K562 cell line was cultured in RPMI-1640 containing 10% heat-inactivated FCS with 1 mM sodium pyruvate, 100 U/ml penicillin, and 100 µg/ml streptomycin. EBV-LCL cells were a kind gift from R. Childs (NIH) and were cultured in RPMI supplemented with 10% fetal bovine [4].

Flow cytometry and cell sorting:

Single-cell suspensions were stained with the appropriate monoclonal antibody in PBS containing 2% FCS. When necessary, intracellular staining was performed by use of the FoxP3/Transcription Factor Staining Buffer Set (eBioscience) according to the manufacturer's instructions. LSRII, Fortessa, (BD Biosciences) were used for cell analysis. Antibodies specific for NK1.1 (PK136; 1:100), CD19 (1D3; 1:400), CD3 (17A2; 1:400 or REA641; Miltenyi Biotec; 1:150); CD122 (TM-β1; 1:200), NKp46 (29A1.4; 1:100), KLRG1 (2F1; 1:200), CD27 (SB/199; 1:200), CD11b (M1/70; 1:200), IL-7R (A7R34; eBioscience; 1:200) CD49b (DX5; 1:100), CD49a (Ha31/8; 1:200) Ly49H (3D10; 1:200) Ly49D (4E5; 1:200), NKG2D (C4; 1:200), NKG2A/C/E (20d5; 1:200), Ly49C/I (5e6; 1:100), CD107a (104B; 1:100) and IFN-γ (XMG1.2; 1:100), DNAM-1 (10E5; 1:200); Ki-67 (AF488; 1:50) were from BD Pharmingen unless stated otherwise.

Cell Counts:

123count eBeads (BD Bioscience) beads were added to single cell suspensions prior to flow cytometry. Cell numbers were enumerated according to manufacturers instructions.

Sample preparation, RNA sequencing and bioinformatics analysis:

RNA isolation from sorted *ex vivo* NK cells was extracted using the RNeasy Plus mini Kit (#74134, QIAGEN, Hilden, Germany), according to the manufacturer's instructions. Purified RNA was measured using an Agilent 2200 TapeStation System (Agilent) with High Sensitivity (HS) RNA ScreenTapes (#5067-5579, Agilent). For Library construction, Full length cDNA were generated from 4 ng of total RNA using Clontech SMART-Seq v4 Ultra Low Input RNA kit for Sequencing (Takara Bio Europe, Saint Germain en Laye, France) according to manufacturer's instructions with 9 cycles of PCR for cDNA amplification by Seq-Amp polymerase. Six hundreds pg of pre-amplified cDNA were then used as input for Tn5 transposon tagmentation by the Nextera XT DNA Library Preparation Kit (96 samples) (Illumina, San Diego, CA) followed by 12 cycles of library amplification. Following purification with Agencourt AMPure XP beads (Beckman-Coulter, Villepinte, France), the size and concentration of libraries were assessed by capillary electrophoresis. The library was sequenced on Illumina Hiseq 4000 sequencer as Single-Read 50 base reads following Illuminas's instruction and base calling were performed using RTA 2.7.7 and bcl2fastq. Approximately 60 million reads per sample were obtained by pooling RNA libraries and performing single-end 50bp sequencing.

Sequencing was performed at the GenomEast platform at the IGBMC (Institut de Génétique et de Biologie Moléculaire et Cellulaire). Single-End reads 35-76bp in length corresponding to *Cish*$^{-/-}$ and WT *Cish*$^{+/+}$ NK cells (3 biological replicates per group) were quality checked using fastqc [5]. Low quality bases (Phred quality score less than 30) were filtered out and TrueSeq Adapters were trimmed using trimmomatic [6]. Reads were mapped to mm10 using subread-align (v1.5.0) [7] with default parameters. The aligned reads were summarized at the gene-level using featureCounts[8], counts were normalized by the size of each library (DESeq2,estimateSizeFactors function) and

finally differentially expressed genes (DEG) analysis was performed using DESeq2 package with default parameters [9]. Genes were considered as DEG if they achieved a false discovery rate of 5% or less. Finally, gene annotation and GO/KEGG pathway enrichment analysis were carried out using Mus musculus (org.Mm.eg.db) AnnotationDbi [10] and clusterProfiler (enrichGO and enrichKEGG functions) [11] packages from R/Bioconductor.

Plasmids

All plasmids used are described in the supplemental material of the paper. pHR-SFFV-KRAB-dCas9-P2A-mCherry [12] was purchased from addgene. sgRNAs targeting *Cish* were designed using the broad institute online tool sgRNA design CRISPR(i) (https://portals.broadinstitute.org/gpp/public/analysis-tools/sgrna-design-crisprai). The sgRNA leading to the most important downregulation of CISH protein in western blot was subsequently used in our study (CISH sgRNA sequence: CTGGAGGGAACCAGTGGGCG). This CISH was then inserted into EF1-GFP-U6 vector using EF1-GFP-U6-gRNA linearized SmartNuclease Lentivector Plasmid kit according to manufacturer's instructions (system biosciences).

NK-92 & primary NK cells transduction

Transduction was performed as previously described and detailed in supplemental material [13]. Briefly, HEK-293T cells were transfected with plasmids encoding for HIV gagpol (psPAX2), and the viral envelopes, VSV-g or BaEV [13] and the plasmid coding for the vector of interest using lipofectamine LTX (Invitrogen). 48hrs later the virus-containing supernatant from HEK-293T cells was concentrated 100-fold using Lenti-X concentrator (Takara). Titration was performed on HEK293T cells (ATCC) using serial vector dilutions. After production, concentrated viruses were added at the indicated MOI (multiplicity of infection) in presence of retronectin at 10ug/ml (Takara). The plates were then centrifuged at 1,000 g for 1 h and incubated at 37°C during 3hrs. NK-92 or primary NK cells were then added at 1. 10^6 cells/ml in 500ul of regular medium supplemented with

IL-2 500UI in presence of protamine-sulfate at 20ug/ml (Sigma). The plates were then centrifuged at 1,000 g for 1 h and incubated at 37°C overnight. The next day, IL-2-supplemented medium was added to each well. Transduction was assessed by cytometry on day 7 after transduction. NK-92 or primary NK cells were then sorted using the the BD *FACSAria™ III* Cell Sorter sorting mCherry and GFP positive cells.

Experimental tumor experiments:

Single-cell suspensions of 3×10^5 B16F10 melanoma cells were injected i.v. into the tail vein of the indicated strains of mice. Mice were sacrificed and lungs were harvested on day 14. Lungs from B16F10 injected mice were fixed in PFA 4% overnight to count B16F10 metastases. E0771-GFP$^+$-Luciferase breast cancer cells were injected into the tail vein of the indicated strains of mice (5×10^5 cells/mouse). Luciferase expression was then monitored at day 7 and 14 by bioluminescence using PhotonIMAGER (BiospaceLab), following intraperitoneal injection of luciferin (30 mg/kg). After completion of the analysis organ luminescence was assessed. Orthotopic implantation of breast tumors was performed as previously described [3]. Briefly, EO771-Luc/GFP cells were suspended in 100 µL of a mixture of PBS/Matrigel (v/v) (Corning). 5×10^5 EO771-Luc/GFP cells were injected into the 4th inguinal mammary fat pads of 6 to 10 week old female C57BL/6 mice. Tumor growth was monitored by caliper measurements and weighted at day 15. Lung and liver were harvested at day 15, Luciferase expression was monitored by bioluminescence using PhotonIMAGER (BiospaceLab), after intraperitoneal injection of luciferin (30 mg/kg). Tumor dissociation was performed as previously described [3], the counting of Infiltrated NK cells was performed using countbright absolute counting beads by flow cytometry (ThermoFisher Scientific, #C36950) according to manufacturer's instructions.

NK-92 Cells adoptive transfer:

For in vivo adoptive transfer experiment 6-8 weeks old NSG female mice were injected in the tail vein at day 0 with $0.2x10^6$ U-937 GFP cells. Mice were i.v. injected with $10x10^6$ human WT transduced NK92 and sgCISH NK-92 cells (n≥6) at days 1, 4, 8, 15 and 17. At day 18, bone marrow (mixed from tibias and femurs) were harvested and the presence of AML blasts (U-937 cell line) was determined by flow cytometry (GFP pos)

Bibliography:

1. Skarnes WC, Rosen B, West AP, et al. A conditional knockout resource for the genome-wide study of mouse gene function. *Nature* 2011;474(7351):337-42. doi: 10.1038/nature10163

nature10163 [pii] [published Online First: 2011/06/17]
2. Narni-Mancinelli E, Chaix J, Fenis A, et al. Fate mapping analysis of lymphoid cells expressing the NKp46 cell surface receptor. *Proc Natl Acad Sci U S A* 2011;108(45):18324-9. doi: 10.1073/pnas.1112064108

1112064108 [pii] [published Online First: 2011/10/25]
3. Karkeni E, Morin SO, Bou Tayeh B, et al. Vitamin D Controls Tumor Growth and CD8+ T Cell Infiltration in Breast Cancer. *Front Immunol* 2019;10:1307. doi: 10.3389/fimmu.2019.01307 [published Online First: 2019/06/28]
4. Lundqvist A, Berg M, Smith A, et al. Bortezomib Treatment to Potentiate the Anti-tumor Immunity of Ex-vivo Expanded Adoptively Infused Autologous Natural Killer Cells. *J Cancer* 2011;2:383-5. doi: 10.7150/jca.2.383 [published Online First: 2011/07/14]
5. Andrews S. FastQC: a quality control tool for high throughput sequence data. http://www.bioinformatics.babraham.ac.uk/projects/fastqc, 2010.
6. Bolger AM, Lohse M, Usadel B. Trimmomatic: a flexible trimmer for Illumina sequence data. *Bioinformatics* 2014;30(15):2114-20. doi: 10.1093/bioinformatics/btu170 [published Online First: 2014/04/04]
7. Liao Y, Smyth GK, Shi W. The Subread aligner: fast, accurate and scalable read mapping by seed-and-vote. *Nucleic Acids Res* 2013;41(10):e108. doi: 10.1093/nar/gkt214

gkt214 [pii] [published Online First: 2013/04/06]
8. Liu Y, Wang L, Han X, et al. The Profile of Timing Dialysis Initiation in Patients with End-stage Renal Disease in China: A Cohort Study. *Kidney Blood Press Res* 2020:1-14. doi: 10.1159/000504671

000504671 [pii] [published Online First: 2020/01/31]
9. Love MI, Huber W, Anders S. Moderated estimation of fold change and dispersion for RNA-seq data with DESeq2. *Genome Biol* 2014;15(12):550. doi: s13059-014-0550-8 [pii]

10.1186/s13059-014-0550-8 [published Online First: 2014/12/18]
10. Carlson MO, Montilla-Bascon G, Hoekenga OA, et al. Multivariate Genome-Wide Association Analyses Reveal the Genetic Basis of Seed Fatty Acid Composition in Oat (Avena sativa L.). *G3 (Bethesda)* 2019;9(9):2963-75. doi: 10.1534/g3.119.400228

g3.119.400228 [pii] [published Online First: 2019/07/13]

11. Yu G, Wang LG, Han Y, et al. clusterProfiler: an R package for comparing biological themes among gene clusters. *OMICS* 2012;16(5):284-7. doi: 10.1089/omi.2011.0118 [published Online First: 2012/03/30]
12. Gilbert LA, Horlbeck MA, Adamson B, et al. Genome-Scale CRISPR-Mediated Control of Gene Repression and Activation. *Cell* 2014;159(3):647-61. doi: 10.1016/j.cell.2014.09.029

S0092-8674(14)01178-7 [pii] [published Online First: 2014/10/14]
13. Colamartino ABL, Lemieux W, Bifsha P, et al. Efficient and Robust NK-Cell Transduction With Baboon Envelope Pseudotyped Lentivector. *Front Immunol* 2019;10:2873. doi: 10.3389/fimmu.2019.02873 [published Online First: 2020/01/11]

Targeting CISH enhances natural cytotoxicity receptor signaling and reduces NK cell exhaustion to improve solid tumor immunity

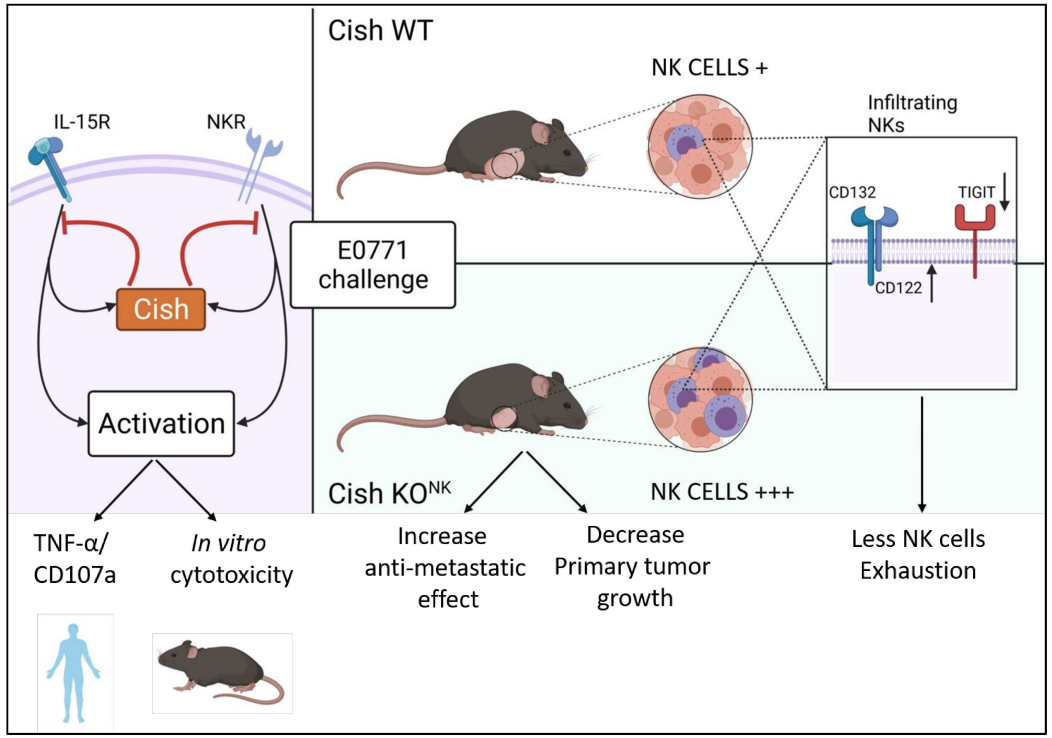

Authors: Bernard, P-L. , Delconte, R. B. , Pastor, S. , Laletin, V. , Costa Da Silva, C. , Goubard, A. , Josselin, E. , Castellano, R. , Krug, A., Vernerey, J. , Devillier R. , Olive, D. , Verhoeyen, E., Vivier, E., Huntington, N. D., Nunès, J. A. and Guittard, G.

Correspondence:
geoffrey.guittard@inserm.fr
Jacques.nunes@inserm.fr

In brief:
Targeting CISH improves NK cells *ex-vivo* proliferation, functions and signaling activation of several pathways such as cytokines and NK activating receptors. *In vivo* CISH absence favors NK cells infiltration to the tumor burden, optimize their killing properties and limits NK cells exhaustion. Consequently, primary tumor and metastasis development are greatly impaired in pre-clinical mouse model. Finally, we targeted CISH in human NK-92 or primary NK cells, using a technology combining the CRISPR(i)-dCas9 tool with a new lentiviral pseudotype, this, improving their function. Our results validate CISH as an emerging therapeutic target to enhance NK cell immunotherapy.